

CHALMERS



Battery Thermal Management Systems of Electric Vehicles

Master's Thesis in Automotive Engineering

JILING LI

ZHEN ZHU

Department of Applied Mechanics

Division of Vehicle Engineering & Autonomous Systems

Road Vehicle Aerodynamics and Thermal Management

CHALMERS UNIVERSITY OF TECHNOLOGY

Göteborg, Sweden 2014

Master's thesis 2014:42

MASTER'S THESIS IN AUTOMOTIVE ENGINEERING

Battery Thermal Management Systems of
Electric Vehicles

JILING LI

ZHEN ZHU

Department of Applied Mechanics
Division of Vehicle Engineering & Autonomous Systems
Road Vehicle Aerodynamics and Thermal Management

CHALMERS UNIVERSITY OF TECHNOLOGY

Göteborg, Sweden 2014

Battery Thermal Management Systems of Electric Vehicles

JILING LI

ZHEN ZHU

©Jiling Li;Zhen Zhu, 2014

Master's Thesis 2014:42

ISSN 1652-8557

Department of Applied Mechanics

Division of Vehicle Engineering & Autonomous Systems

Road Vehicle Aerodynamics and Thermal Management

Chalmers University of Technology

SE-412 96 Göteborg

Sweden

Telephone: + 46 (0)31-772 1000

Cover:

Saab 9-3 ePower electric vehicle made its debut at 2010 Paris Motor Show

Chalmers / Department of Applied Mechanics

Göteborg, Sweden 2014

Battery Thermal Management Systems of Electric Vehicles

Master's Thesis in *Automotive Engineering*

JILING LI

ZHEN ZHU

Department of Applied Mechanics

Division of Vehicle Engineering & Autonomous Systems

Road Vehicle Aerodynamics and Thermal Management

Chalmers University of Technology

ABSTRACT

Electric vehicles (EV) develop fast and have become popular due to their zero emission and high tank-to-wheels efficiency. However, some factors limit the development of the electric vehicle, especially performance, cost, lifetime and safety of the battery. Therefore, the management of batteries is necessary in order to reach the maximum performance when operating at various conditions.

The battery thermal management system (BTMS) plays a vital role in the control of the battery thermal behaviour. The BTMS technologies are: air cooling system, liquid cooling system, direct refrigerant cooling system, phase change material (PCM) cooling system, and thermo-electric cooling system as well as heating. These systems are analysed through a trade-off between performance, weight, size, cost, reliability, safety and energy consumption. According to the analysis two prime battery thermal management systems are recommended: combined liquid system (CLS) and a variant system with PCM.

The models of CLS and PCM system were built and simulated using software MATLAB/Simulink. The simulation results predict the battery temperature variation and the energy consumption of BTMS. Through simulating the PCM system model, the effect of PCM on battery temperature variation was investigated and the proper PCM mass was estimated.

Seen from the simulation results, BTMS is of great importance to control battery thermal behaviour. Further study could be more comprehensive and accurate through combining the simulation model with battery thermal electric and CFD models.

Key words: EV, Battery thermal management, BTMS, Air cooling system, Liquid cooling system, Direct refrigerant system, PCM, MATLAB/Simulink model

Contents

1	INTRODUCTION	1
1.1	Background	1
1.2	Objectives	1
1.3	Limitation	1
1.4	Thesis Outline	2
2	THEORY	3
2.1	Lithium-ion Battery	3
2.1.1	Mechanism of Secondary Lithium-ion battery	3
2.1.2	Thermal Issues of Li-ion battery	4
2.1.3	Operating Requirements	5
2.2	Heat Transfer	7
2.2.1	Overall Heat Transfer Coefficient	7
2.2.2	Heat Balancing within Heat Exchanger	9
2.3	On-Off Controller	10
2.4	Phase Change Material (PCM)	12
3	BATTERY THERMAL MANAGEMENT SYSTEMS (BTMS)	13
3.1	Systems Functions	13
3.2	Technologies of BTMS	14
3.2.1	Air Cooling and Heating	14
3.2.2	Liquid Cooling and Heating	15
3.2.3	Direct Refrigerant Cooling and Heating	16
3.2.4	PCM	17
3.2.5	Thermoelectric Module	17
3.2.6	Heat Pipe	18
3.2.7	PTC Heater	19
3.3	Evaluation of Different Technologies	19
3.3.1	Forced Air System	19
3.3.2	Liquid System	20
3.3.3	PCM System	20
3.3.4	Thermo-electrics	21
3.4	Recommended Cooling System	22
3.4.1	Combined Liquid System (CLS)	22
3.4.2	PCM Model (CLS+PCM)	23
4	MODELLING OF BTMS	24
4.1	Modelling Conditions	25
4.2	CLS Model	27
4.2.1	Battery Unit	27

4.2.2	Air Conditioner (Active Cooling)	28
4.2.3	Radiator (Passive Cooling)	28
4.2.4	PTC Heater (Heating)	29
4.2.5	Pump	29
4.2.6	Control Unit	31
4.3	PCM Model	33
4.4	Performance Parameters	34
5	RESULTS AND DISCUSSION	36
5.1	CLS Model	36
5.1.1	NEDC versus US06	39
5.1.2	Cold and Hot Weather	40
5.1.3	Mild Weather	44
5.2	PCM Model	45
5.2.1	Comparison of Two Systems	45
5.2.2	Choose the PCM Mass	46
6	CONCLUSION	49
7	FUTURE PROSPECTS	50
	REFERENCES	52
	APPENDIX A: SYSTEM EVALUATION	54
	APPENDIX B: MODELLING PROCESS	57
	APPENDIX C: CLS RESULTS	59
	APPENDIX D: CLS+PCM RESULTS	63

Acknowledgements

It is our honour to be involved in this master thesis project. Experts at LeanNova Engineering AB have been very welcoming, friendly and helpful throughout our thesis. They have continuously supported us with their comprehensive expertise and knowledge of automotive systems. We have gained a lot from this thesis not only the experience but also the innovate spirit to solve complex problems.

We would like to extend a warm thank you to our supervisor Peter Hayden who has been involved in most of this thesis. With his expertise for HVAC system, we have managed to solve dozens of problems. He also inspired us with ideas, action and confidence by talking with us patiently. The project would never have completed without his engineering skills and management.

Thank you also to all our great team members. Zhongyuan Zhang has provided us strong theoretical support in thermodynamic, MATLAB simulation and battery technology. Her guidance took us directly into the central issues without detour. Claes Zimmer and Anders Lindén have accompanied us from the beginning to the end with their knowledgeable comments and answers to all our questions.

We would also like to thank our examiner Professor Lennart Löfdahl. In weekly conversation during the project he has brought us his guidance and advice in every aspect.

Lastly, we would like to thank our friends and our family for all support and encouragement throughout the project and also our study in Chalmers.

Jiling Li and Zhen Zhu

Göteborg, 2014

Notations

Symbol List

A	(Contact) area
Li	Lithium
q	Heat transfer rate
\dot{Q}_{gen}	Heat generation rate
\dot{Q}_{dis}	Heat dissipation rate
Re	Reynolds number
T_{amb}	Ambient temperature
T_{ba}	Battery temperature
$T_{ba,in}$	Battery initial temperature
T_{des}	Desired temperature
$T_{fl,in}$	Fluid inlet temperature
$T_{fl,out}$	Fluid outlet temperature
ΔT_M	Mean temperature difference
U	Overall heat transfer coefficient

Abbreviation List

AC	Air Conditioner / Air Conditioning
BEV	Battery Electric Vehicle
BMS	Battery Mangement System
BP	Bypass
BTMS	Battery Thermal Management System
Eq.	Equation
EV	Electric Vehicle
Fig.	Figure
HT	Heater / Heating
HVAC	Heating, Ventilation and Air Conditioning
kph	kilo per hour
NEDC	New European Driving Cycle
P	Page
PCM	Phase Change Material
PTC	Positive Temperature Coefficient
RA	Radiator
Sec.	Section
SEI	Solid electrolyte interface/interphase
Tab.	Table
TDC	Testing Driving Cycle
US06	A Supplemental Federal Test Procedure of USA

1 Introduction

In this chapter, a brief synopsis of this report is presented. Section 1.1 Background, explains the original motivation of this thesis. Section 1.2 Objectives, points out what this thesis is aiming at. Section 1.3 Limitation, defines the circumscription of thesis work and Section 1.4 Thesis Outline, introduces briefly the report structure.

1.1 Background

There are nowadays different blending levels of hybrid electric vehicle and pure electric vehicle available on the current automobile market. According to the blending level, various size, type and number of battery cells are mounted in EVs. Unlike conventional fuel, battery cells as an energy source have stricter requirement on working environment. They are especially sensitive to temperature. To ensure a proper thermal working environment, a Battery Thermal Management System (BTMS) will normally be integrated with battery cells. Thus, knowledge about the proper working requirements of battery is vital, and what kind of management systems can sufficiently and efficiently meet these requirements. With this cornerstone, the performance and durability of battery pack can be maximized in an electric vehicle. Furthermore, the electric range of vehicle is restricted due to limited capacity of the battery. It is very useful to investigate carefully the electric energy consumption of BTMS and to look for potential savings. This investigation will help battery performance by reducing the energy consumption of BTMS and extending the electric range of EVs.

1.2 Objectives

The main purpose of this master thesis is to develop a BTMS model for balancing the different cooling and heating circuits within the battery pack to fulfil the performance requirements. As prerequisites for the modelling, the requirements of the battery pack will be investigated at first through literature research. Then, several potential BTMSs, both in commercial stage and study phase, will be listed in a concept selection matrix with their pros and cons. Two of them will be proposed as candidates for the following simulation. After the models are built up through simulation tool Simulink®, they will be tested in different initial conditions. Lastly, the corresponding performance parameters of systems will be analysed and compared.

1.3 Limitation

Although hybrid EVs are popular on the current market, this thesis concentrates only on battery electric vehicles and plug-in hybrid electric vehicles which are equipped with larger battery packs compared with those on other EVs. The thesis focuses only on building a simulation model for the thermal balancing within the battery pack. Thus, the exact heat generation model of battery cells is not discussed in detail; also this model is taken from an exterior resource. Furthermore, the other cooling and heating circuits, such as chiller, radiator and heater, will be simplified. The delay, fluctuation or fading of operation will be neglected. The pre- and post-conditions will be mentioned, but the operation and system feature during test driving cycles is the main points of this thesis and thus will be intensively investigated and compared.

1.4 Thesis Outline

This report is divided into seven main chapters. It starts with a general introduction in Chapter 1 and a theoretical fundamental in Chapter 2 which offers basic knowledge about Li-ion battery, heat transfer theory, on-off control and PCM. Chapter 3 presents the basic required functions of BTMS and several commercial and potential solutions in Section 3.2 with corresponding evaluation in Section 3.3. Depending on the evaluation two candidate systems are proposed in Section 3.4.

Based on the system description in Chapter 4 the combined liquid system model is built up at the first phase in Section 4.1. Then improvement is achieved with an additional PCM unit which is described in Section 4.2. Chapter 5 presents the modelling results of both systems with defined performance parameters.

In the Chapter 6 a final conclusion based on previous results analysis is discussed. Lastly, possible work for the future is recommended for completing and optimising the models.

To summarise the contributions: Jiling Li took main responsibility for Sections 2.1 2.4 3.3 3.4 4.2.4 4.2.5 4.3 5.2; and Zhen Zhu took main responsibility for Sections 2.2 2.3 3.2 4.1 4.2.1-4.2.3 4.2.6 5.1. The rest of the report was completed in co-operation with each other.

2 Theory

This chapter highlights the most important fundamental points of thesis, presenting the theoretical thoughts of automobile engineering, chemistry, thermodynamics and automatic control behind numerical simulations.

2.1 Lithium-ion Battery

2.1.1 Mechanism of Secondary Lithium-ion battery

A lithium-ion battery consists of an anode, cathode and electrolyte as well as a separator, see Figure 2.1. The anode, is the oxidised electrode which removes electrons to the external circuit during discharging. Correspondingly, the cathode, is the oxidising electrode which receives electrons from the external circuit. The electrolyte is the medium to transfer ions between electrodes inside the cell and the separator is used to isolate electrodes. Also, the solid electrolyte interface (SEI) is thin passivation layer which is formed on the surface of the carbon anode during the first charge. It slows down the reaction rate and decreases the current. (electropaedia, 2014)

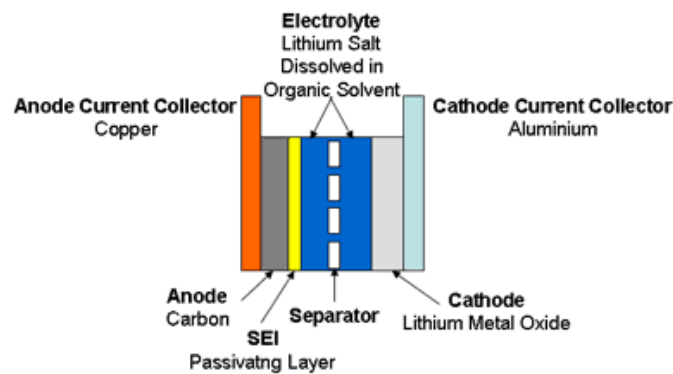
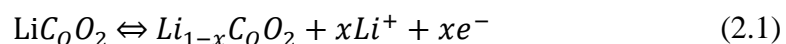


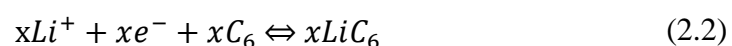
Figure 2.1 The physical structure of lithium-ion battery (electropaedia, 2014)

Secondly a Li-ion battery is rechargeable which means its electrochemical reactions are reversible. Lithium ions disperse from the negative to the positive when discharging and go in reverse when charging. Lithium-ion battery use intercalated lithium compound as the electrode instead of metallic lithium. The electrochemical reactions for Li-cobalt in the positive electrode and negative electrode are expressed as following:

The positive electrode reaction is:



The negative electrode reaction:



The electrochemical reactions in the positive electrode and negative electrode for other lithium batteries are similar.

There are many types of lithium-ion battery which are named by cathode oxides and each one has its own characteristics as followings:

Table 2.1 Reference names for Li-ion batteries (Battery University, 2014).

Chemical name	Material	Short form	Note
Lithium Cobalt Oxide	LiCoO ₂	Li- cobalt	High capacity; for cell phone laptop, camera
Lithium Manganese Oxide	LiMn ₂ O ₄	Li- manganese	Most safe; lower capacity than Li-cobalt but high specific power and long life. Power tools, e-bikes, EV, medical, hobbyist.
Lithium Iron Phosphate	LiFePO ₄	Li- phosphate	
Lithium Nickel Manganese Cobalt Oxide	LiNiMnCoO ₂	NMC	
Lithium Nickel Cobalt Aluminium Oxide	LiNiCoAlO ₂	NCA	Gaining importance in electric powertrain and grid storage
Lithium titanate	Li ₄ Ti ₅ O ₁₂	Li- titanate	

Seen from Table 2.1, three types of lithium batteries are particularly suitable for an EV battery, namely LiMn₂O₄, LiFePO₄, and LiNiMnCoO₂.

2.1.2 Thermal Issues of Li-ion battery

Lithium-ion cells performance depends on both the temperature and the operating voltage. Lithium-Ion cells work well when cells operate within limited voltage and temperature. Otherwise, damage will occur to the cells and will be irreversible.

In over-voltage situations the charging voltage exceeds the bearable cell voltage, resulting in excessive current flows and at the same time, it causes two problems.

At excessive currents the Lithium-ions are deposited more rapidly than intercalation to the anode layers, Lithium ions are then deposited on the surface of the anode as metallic Lithium. This is Lithium plating. It gives rise to the reduction in the free Lithium ions and an irreversible capacity loss. (Electropaedia, 2014). There are two types of metal lithium plating, namely homogeneous lithium plating and heterogeneous lithium plating, but the lithium plating is dendritic in form. Eventually it can result in a short-circuit between the electrodes.

As with over-voltage, under-voltage also brings about problems which give rise to the breakdown of the electrode materials.

For the anode, the copper current collector breaks down. It causes the increase of battery discharge rate and battery voltage, however, the copper ions are precipitated as metal copper which is irreversible. The situation is dangerous for it can result in short-circuit between anode and cathode. For the cathode, the cobalt oxide or manganese oxide will be decomposed after many cycles under low voltage. Meanwhile, oxygen will be released and the battery suffers from capacity loss.

The battery temperature should be controlled carefully. Both excess heat and lack of heat will bring about problems.

Chemical reaction rates have a linear relation to temperature. The decrease of the operating temperature will reduce reaction rate and the capacity of carrying current during charging or discharging. In other words, the battery power capacity is decreased. Moreover, the reduction of reaction rate makes it harder to insert lithium ions into intercalation spaces. The result is the reduction of power and lithium plating causing the capacity loss.

High temperature increases the reaction rate with higher power output, however, it also increases the heat dissipation and generates even higher temperatures. Unless heat is dissipated quicker than heat is generated, the temperature will be higher and finally a thermal runaway will result.

Thermal runaway consists of several stages and each stage will give rise to more irreversible damage to cells. First, the SEI layer is dissolved to electrolyte at around 80 °C. The primary overheating may result from excessive current or high ambient temperature. After breakdown of the SEI layer, electrolyte begins to react with the anode. This reaction is exo-thermal which drives the temperature higher. Secondly, the higher temperature causes the organic solvents to break down with the release of hydrocarbon gases. Normally this starts at around 110 °C. The pressure inside cells is built up by the gas and the temperature is beyond the flashpoint. However, the gas does not burn due to the lack of oxygen. A vent is needed to release the gas in order to keep cells under proper pressure and avoid a possible rupture. Then, the separator is melted and short-circuits occur between the anode and cathode at 135 °C. Finally, the metal-oxide cathode breaks down at 200 °C and releases oxygen which allows the electrolyte and hydrogen gas to burn. This reaction is also exo-thermal and drives temperature and pressure still further. (Electropaedia, 2014)

In addition, uneven temperature distribution is another problem of batteries. Typically, it is caused by the excessive local temperature, variable current in a cell and the thermal conductivity of the case, as well as the placement of positive and negative terminals and so on. (Pesaran, 2001) It results in local deterioration and even thermal runaway with reducing the battery lifetime. (Kizilel, et al., 2009)

2.1.3 Operating Requirements

The battery temperature should be controlled within temperature limits to avoid the thermal issues and improve the performance. The temperature range affects the battery power and battery cycle life, see Figure 2.2 and Figure 2.3. At the same time, the temperature distribution should be even to guarantee the battery performance and

lifetime. That is also the reason why the battery thermal management system is necessary to the battery system.

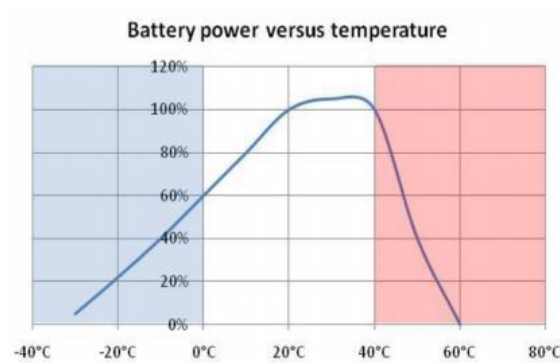


Figure 2.2 Battery power and temperature (Matthe, et al., 2011).

When temperature ranges from 20 °C to 40 °C, battery power reaches maximum, see Figure 2.2.

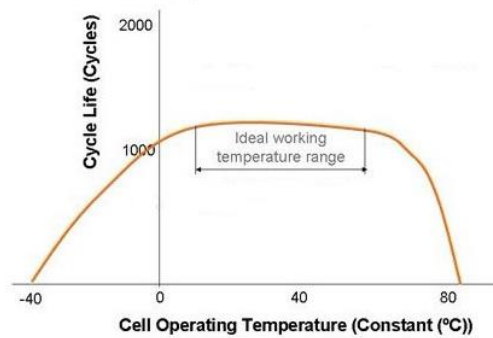


Figure 2.3 Cycle life and temperature (Electropaedia, 2014).

The cycle life goes down slowly below 10 °C because of anode plating and drops off quickly above 60 °C due to the breakdown of electrode materials, see Figure 2.3.

Generally, the temperature must be controlled between 20 °C and 40 °C to ensure the performance and cycle life. Moreover, the temperature distribution is controlled under 5K to keep the safety and lifetime of battery (Pesaran, 2002). In addition, ventilation is also essential to the battery system and should be taken into account.

2.2 Heat Transfer

2.2.1 Overall Heat Transfer Co-efficient

To predict the performance of the heat exchange, the heat transfer can generally be expressed using overall heat transfer co-efficient by following equation (Incropera, 2007, p. 678):

$$q = UA\Delta T_M \quad (2.3)$$

where

- q Heat transfer rate [W]
- U Overall heat transfer coefficient [W/ (m²K)]
- A Heat transfer surface area [m²]
- ΔT_M Approximate mean temperature different [K]

This equation includes the convective and conductive parts of heat transfer between the hot and cold fluids in the heat exchanger. The radiation part of heat transfer and the heat transfer between the heat exchanger and the atmosphere is negligible.

For the un-finned, tubular heat exchanger of Figure 2.4, the overall heat transfer co-efficient can be expressed as Equation 2.4 (Incropera, 2007, p. 675)

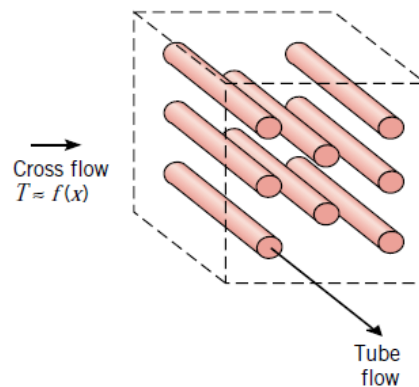


Figure 2.4 Un-finned, tubular cross-flow heat exchanger (Incropera, 2007, p. 671).

$$\frac{1}{UA} = \frac{1}{h_i A_i} + \frac{R''_{f,i}}{A_i} + R_w + \frac{R''_{f,o}}{A_o} + \frac{1}{h_o A_o} \quad (2.4)$$

where

- UA Product of U and A [W/K], A could be either A_i or A_o .
- h_i, h_o Convective heat transfer co-efficient of inner, outer tube surface [W/m²K]
- A_i, A_o Contact area of inner, outer tube surface [m²]
- $R''_{f,i}, R''_{f,o}$ Fouling Factors [m²K/W]

R_w Conductive resistance [K/W]

R_w in this case indicates the conductive resistance of the tube and is obtained by the equation $\frac{\ln(D_o/D_i)}{2\pi kL}$ where D_o is the outer diameter of the tube, D_i is the inner diameter, k is the thermal conductivity of the tube material, and L is the tube length

In particular, if the convection of outer surface occurs very strong i.e. $h_o \rightarrow \infty$ and the fouling effect is insignificant, the terms $\frac{1}{h_o A_o}$, $\frac{R''_{f,i}}{A_i}$ and $\frac{R''_{f,o}}{A_o}$ in Equation 2.4 can be negligible and the equation reduces to

$$\frac{1}{UA} = \frac{1}{h_i A_i} + \frac{\ln(D_o/D_i)}{2\pi kL} \quad (2.5a)$$

If the calculation is based on the inner tube surface $A = A_i$ and since $A_i = \pi L D_i$, the Equation 2.5a is equivalent to

$$\frac{1}{U} = \frac{1}{h_i} + \frac{D_i \ln(D_o/D_i)}{2k} \quad (2.5b)$$

or

$$U = \frac{1}{\frac{1}{h_i} + \frac{r_i \ln(r_o/r_i)}{k}} \quad (2.5c)$$

where r_o, r_i refers to the outer and inner tube radius. The Equation 2.5c will be applied in the following model unit ‘‘Battery Pack’’ in Section 4.2.1 to describe the heat transfer between battery cells and heat transfer fluid.

In Equation 2.5a to 2.5c, there is still one parameter unknown which is h convective heat-transfer co-efficient. It can be obtained by the following equations:

$$Nu_D = \frac{h_{fl} \cdot D_h}{k_{fl}} \quad (2.6)$$

where D_h is hydraulic diameter that is equal to D_i in the case of a filled round tube, k_{fl} is the thermal conductivity of fluid and Nu_D is determined according to the different flow situations (laminar or turbulent) (Incropera, 2007, pp. 507,515):

$$\text{laminar: } Nu_D = 3.66 \quad (Re_D \lesssim 3000) \quad (2.7a)$$

$$\text{turbulent: } Nu_D = \frac{(f/8)(Re_D - 1000)Pr}{1 + 12.7(f/8)^{1/2}(Pr^{2/3} - 1)} \quad (3000 \lesssim Re_D \lesssim 5 \times 10^6) \quad (2.7b)$$

In Equation 2.7b Re_D is the Reynolds number, which is determinate by (Incropera, 2007, p. 487)

$$Re_D = \frac{4\dot{m}}{\pi D_h \mu} \quad (2.8)$$

\dot{m} refers to the mass flow-rate of fluid, and μ is the dynamic viscosity of fluid.

f is called the Moody friction factor, which is determinate by (Incropera, 2007, p. 490)

$$f = (0.790 \ln Re_D - 1.64)^{-2} \quad (2.9)$$

Pr is the Prandtl number interpreting the ratio of the momentum and thermal diffusivities and defined by the equation $Pr = \frac{\mu C_p}{k}$.

To combine the equations from 2.6 to 2.9, it can be concluded that for a fixed physical layout and determined fluid the h_{fl} is a function only of \dot{m} which is expressed as:

$$\text{laminar: } h_{fl} = \text{constant} \quad (2.10a)$$

$$\text{turbulent: } h_{fl} = f(\dot{m}) \quad (2.10b)$$

The flow situation is determined by \dot{m} itself. This calculation will be executed in the model unit “Battery Unit” in Section 4.2.1.

2.2.2 Heat Balancing within Heat Exchanger

For a controlled volume the conservation of energy is stated in the expression as (Incropera, 2007, p. 15):

$$\frac{dE_{st}}{dt} = \dot{E}_{in} - \dot{E}_{out} + \dot{E}_g \quad (2.11)$$

The term E_{st} means stored thermal and mechanical energy, \dot{E}_g is the thermal energy (heat) generation rate, \dot{E}_{in} and \dot{E}_{out} are the thermal and mechanical energy transport rate across the control surfaces as inflow and outflow.

To consider the tube of a tube-and-shell heat exchanger as a control volume (see Figure 2.4), the mechanical energy changes can be negligible and the stored thermal energy change will be indicated by temperature change of heat-transfer fluid within the tube.

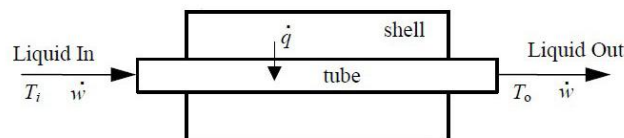


Figure 2.5 Tube-and-shell heat exchanger schematic (Ricker, 2014).

The Equation 2.11 reduces to the following form of the steady-flow energy equation (Ricker, 2014):

$$mC_p \frac{dT_o}{dt} = \dot{m}C_p(T_i - T_o) + \dot{q} \quad (2.12)$$

where

- m Fluid mass within the tube ($= \rho_{fl}V_{fl}$) [kg]
- \dot{m} Fluid mass flow rate through the heat exchanger [kg/s]
- T_i, T_o Temperature of fluid entering and leaving tubes [°C]
- C_p Specific thermal capacity of fluid [J/ (kg K)]
- \dot{q} Heat transfer rate to the liquid in the tube [W]

Note that this equation is widely applicative to different heat transfer situations, such as heater, radiator and chiller. For a heater, \dot{q} refers to the heater power, and for a radiator refers to the heat rejection rate according to the performance diagram.

2.3 On-Off Controller

In many applications, it is required to control a quantity to stay at some fixed value, such as temperature of hot water in a tank. On-off control is one basic mode of control to solve this problem. It is also known as “bang-bang” control, relay control or two-position control. An automatic temperature control might consist of a heater, an actuator and a thermostat. The thermostat measures the water temperature in the tank and activates the actuator to switch on the heater, when heating is required and deactivated the actuator conversely. Consider that, if the switching point of thermostat was 60 °C which is the required temperature of hot water, the system would never work properly, because the heater would be switched on and off rapidly.

To avoid that issue, the thermostat would have two switching points. One upper switching point (might be 61 °C) to shut down the heater, and the other lower switching point (might be 59 °C) to start the heater. Thus, there is a switching difference in the thermostat of 2 °C. Figure 2.6 shows the status of the heater versus the water temperature under the on-off controlling of the thermostat. When the water temperature is at the lower switching temperature (59 °C) or below, the thermostat will activate the heater and keep it working till water temperature reach the upper switching temperature (61 °C). When the water temperature is at the upper switching temperature or above, the thermostat will turn the heater off and keep it off till the lower switching temperature.

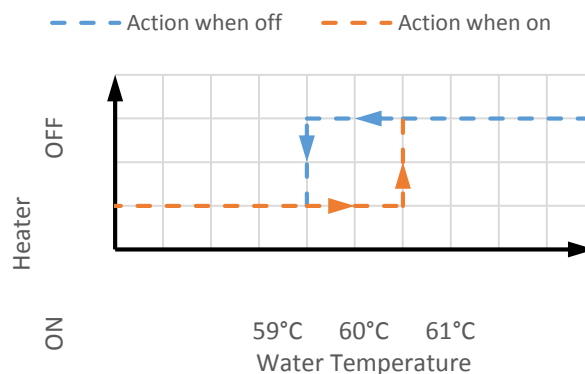


Figure 2.6 Heater action over the water temperature.

To clarify the control feature, Figure 2.7 presents the water temperature in the tank over time. During T_1 the heater is off. At point A the water temperature is at the lower switching point ($59\text{ }^\circ\text{C}$) and the heater is turned on and keeps working during T_2 . At point B the water temperature reaches the upper switching point ($61\text{ }^\circ\text{C}$) and the heater is turned off. However, the heater is still hotter than the water and continues to give up its heat till point C. Due to heat dissipation to the surroundings the temperature decreases subsequently. At point D the heater is active again, because of the delay of warming up, the temperature rise starts at point E later than D.

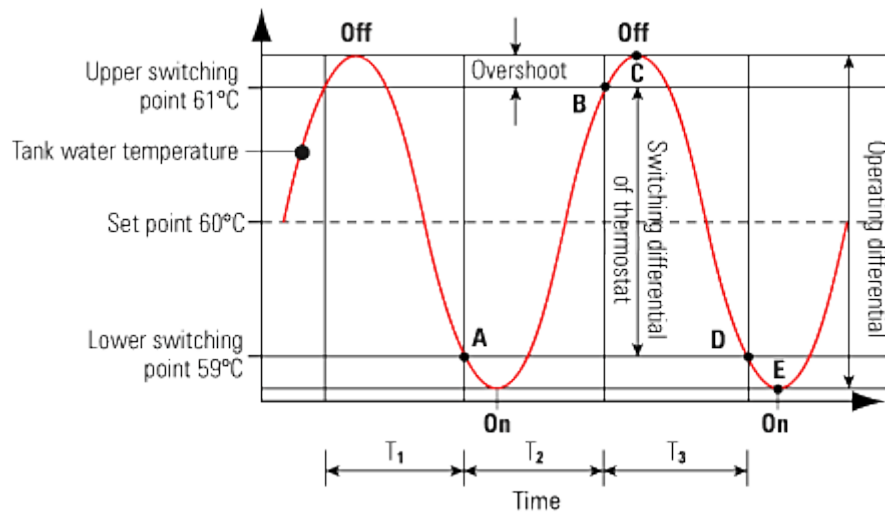


Figure 2.7 Tank temperature versus time (Spirax Sarco, 2011).

The example above shows an on-off controlling system with a single on-off controller, which makes the system possible to switch between two statuses over temperature. In Section 4.1.6 a combination strategy with a three on-off controller will be applied in order to realise a more complex switching between four working conditions.

2.4 Phase Change Material (PCM)

Phase change materials (abbreviated to PCM) has high fusion heat which stores and releases the amount of heat during melting and solidifying at a fixed point. As seen in Figure 2.8, when the temperature is lower than the melting point, PCM is solid and heat is absorbed as sensible heat with the temperature rise. When the temperature reaches the melting point, heat is absorbed and stored as latent heat until the latent heat is up to the maximum without the temperature increasing. At the same time PCM changes its phase from solid to liquid. After that, PCM becomes liquid and heat is absorbed by PCM and stored as sensible heat, see Figure 2.8. The melting temperature of PCM is variable and can be chosen according to requirements.

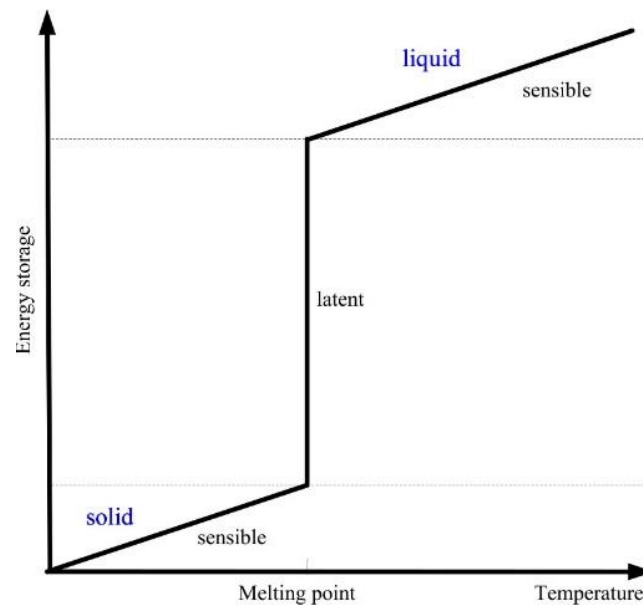


Figure 2.8 The relationship of temperature and energy storage of PCM.

3 Battery Thermal Management Systems (BTMS)

3.1 Systems Functions

As stated in Section 2.1.2 and 2.1.3, the battery pack for safety, performance (both power and capacity) and lifespan reasons should be stored in a controlled surrounding where the temperature is controlled and there is no risk of thermal runaway. According to a foundational research (Pesaran, 2001), the BTMS should be equipped with four essential functions to ensure the right operation conditions of the battery pack:

1. Cooling

Due to inefficiency, battery cells will not only generate electricity but also heat. This heat should be moved from the battery pack when battery temperature reaches the optimum temperature or even in advance. Thus, a cooling function is required in BTMS.

2. Heating

In cold climates, battery pack temperature probably falls below the lower temperature limit. Hence, a heating function, such as PTC heater, is required to assist the battery pack to reach the proper temperature range in a shorter time.

3. Insulation

In extreme cold or hot weather, the temperature difference between the inside and outside of the battery pack is much larger than that in mild weather. Battery temperature will thus fall (cold) or rise (hot) sooner out of the proper temperature range. To prevent this, good insulation can slow down the falling or rising of battery temperature, especially when the vehicle is parked outdoors.

4. Ventilation

Ventilation is required to exhaust the hazardous gases within battery pack. In some systems, such as air systems, this function is combined with cooling and heating functions.

In the following sections, different technologies of heating and cooling will be introduced in detail and their possibility and ease of ventilation will be evaluated. Insulation affects mainly stationary conditions rather than driving conditions, so it will not be further discussed in this thesis.

3.2 Technologies of BTMS

3.2.1 Air Cooling and Heating

Air systems use air as the thermal medium. The intake air could be direct either from atmosphere or from the cabin and could also be conditioned air after a heater or evaporator of an air conditioner. The former is called passive air system and the latter is active air system. Active systems can offer additional cooling or heating power. A passive system can offer some hundreds of watts cooling or heating power and an active system power is limited to 1 kW. (Valeo, 2010)

Because in both cases the air is supplied by a blower, they are also called forced air systems. The following figure shows a schematic description of systems.

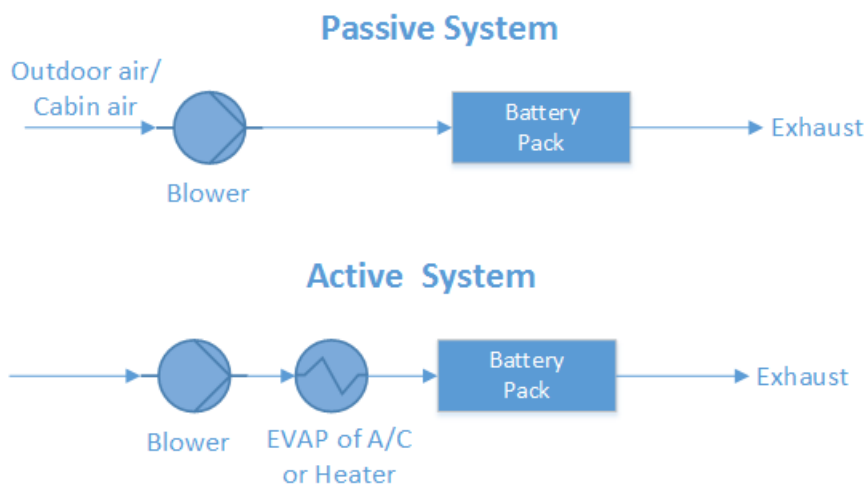


Figure 3.1 Forced air systems (passive and active).

Note that the air system offers full functions of heating, cooling and ventilation. There is no need to build an additional ventilator, but it must be noted that the exhaust air cannot be returned to the cabin again. In some cases, a heat recovery unit (air-air heat exchanger) is mounted after the battery pack in order to recovery the heat from the exhaust air. It can prevent mixture of exhaust air with intake air and at the same time provide an extra saving potential. The forced air system with heat recovery is presented below.

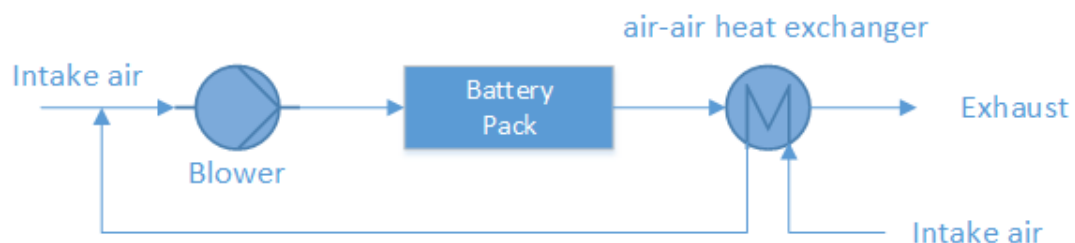


Figure 3.2 Forced air system with heat recovery.

3.2.2 Liquid Cooling and Heating

Besides air, liquid is another heat transfer fluid to transfer heat. There are generally two groups of liquids applied for thermal management systems. One is dielectric liquid (direct-contact liquid) which can contact the battery cells directly, such as mineral oil. The other is conducting liquid (indirect-contact liquid) which can only contact the battery cells indirectly, such as a mixture of ethylene glycol and water. Depending on the different liquids, different layouts are designed. For direct-contact liquid, the normal layout is to submerge modules in mineral oil. For indirect-contact liquid, a possible layout can be either a jacket around the battery module, discrete tubing around each module, placing the battery modules on cooling/heating plate or combining the battery module with cooling/heating fins and plates. (Pesaran, 2001) Between these two groups, indirect contact systems are preferred in order to achieve better isolation between battery module and surroundings and thus better safety performance.

By different heat-sinks for cooling, liquid systems can also be categorized into either passive systems or active systems. In passive liquid system, the heat-sink for cooling is a radiator. This system has no ability to heat. Figure 3.3 presents the systematic scheme of a passive liquid system. Heat transfer fluid is circulated by the pump within a closed system. The circulating fluid absorbs heat from battery pack and releases heat via a radiator. The cooling power depends strongly on the temperature between ambient air and battery. Fans behind the radiator can improve the cooling performance, but if ambient air is higher than the battery temperature or the difference between them is too small, the passive liquid system becomes ineffective.

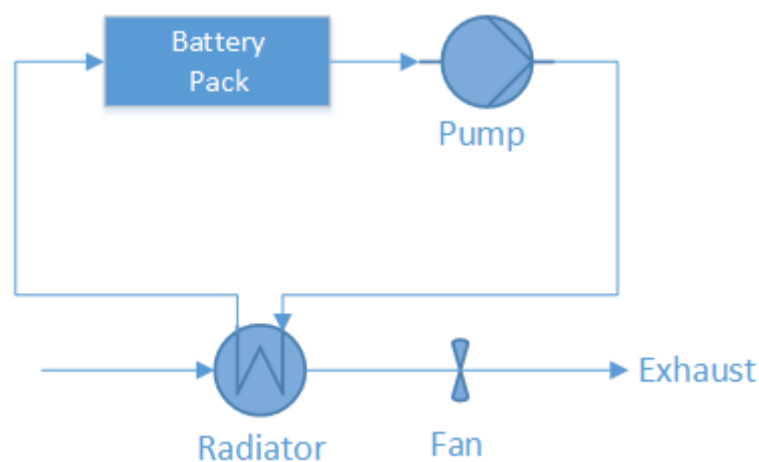


Figure 3.3 *Passive liquid cooling system.*

Figure 3.4 shows the systematic scheme of an active liquid system. There are two loops. The upper is called the primary loop and the lower the secondary loop. The primary loop is similar to the loop in a passive liquid system, where the heat transfer fluid is circulated by pump. The secondary loop is actually an air conditioning loop (A/C loop). The upper heat exchanger instead of being a radiator works as an evaporator (EVAP) for cooling operation and connects both loops. During heating operation, the 4 way valve will be switched, and the upper heat exchanger works as a condenser (COND) and the lower heat exchanger works as an evaporator. The heating operation loop is also called heat pump loop.

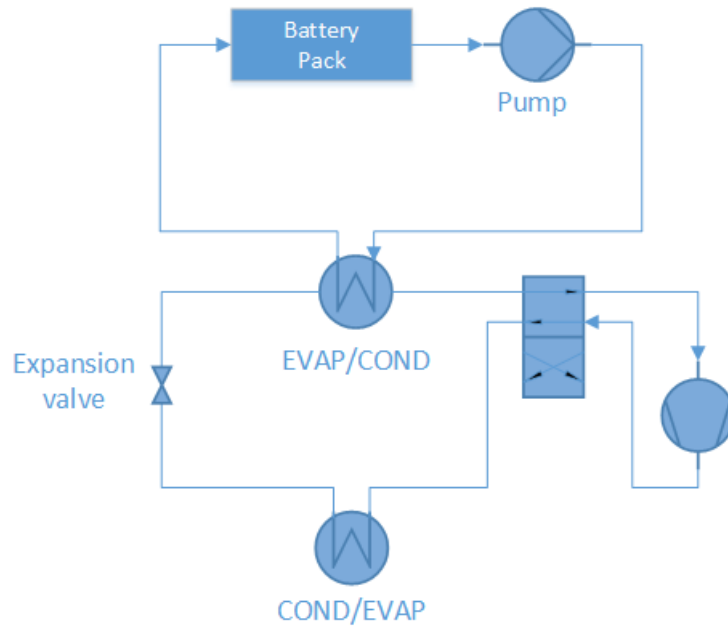


Figure 3.4 Active liquid cooling system.

3.2.3 Direct Refrigerant Cooling and Heating

Similar to active liquid systems, a direct refrigerant system (DRS) consists of an A/C loop, but DRS uses refrigerant directly as heat transfer fluid circulating through battery pack. The systematic layout is in Figure 3.5.

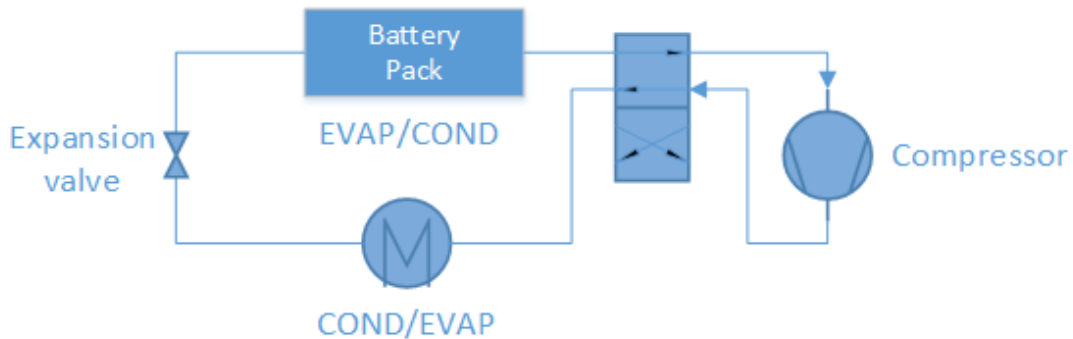


Figure 3.5 Direct refrigerant cooling system.

3.2.4 PCM

During melting, heat is absorbed by PCM and is stored as latent heat until the latent heat is up to the maximum. The temperature is kept at melting point for a period and the temperature increase is delayed. Therefore, PCM is used as conductor and buffer in battery thermal management systems. Figure 3.6 shows the working mechanism of PCM on battery cells. Also, a PCM is always combined with air cooling system or liquid cooling system to manage the battery temperature.

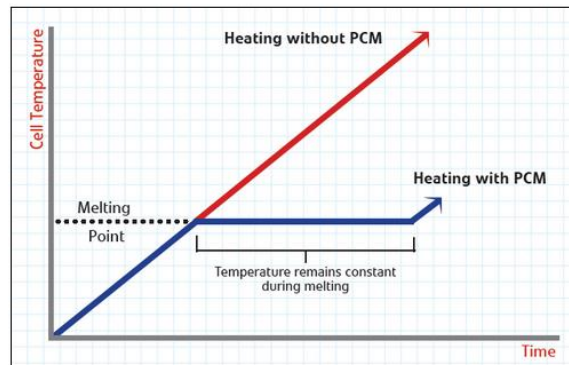


Figure 3.6 The working mechanism of PCM on battery cells (Charged, 2014).

3.2.5 Thermo-electric Module

To improve cooling/heating power of passive air systems, there are two possible upgrades. One is through thermo-electric modules, which will be introduced here. The other is a heat pipe will be discussed in Section 3.2.6.

Thermo-electric module can convert electric voltage to temperature difference and vice-versa. Here the former effect is adopted. That means it transfers heat through the module by consuming electricity directly. The schematic structure is presented in Figure 3.7. Two fans are installed to improve heat transfer by forced convection. To combine a passive air system with thermo-electric module, the combined system is able to cool down the battery even lower than the intake air temperature, but the power is still limited to around some hundreds of watts and less than one kW. (Valeo, 2010) It's easy to switch between cooling and heating operation. To achieve that, the poles of electrodes need to be reversed.

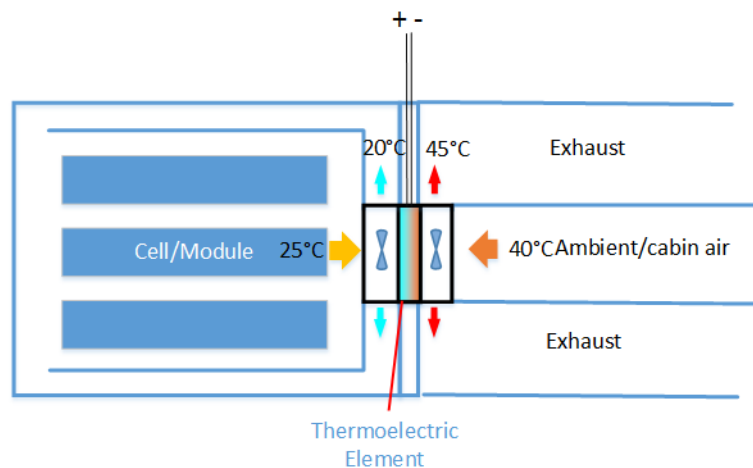


Figure 3.7 Thermo-electric cooling/heating system.

3.2.6 Heat Pipe

Besides thermo-electric modules, a heat pipe is another way to upgrade passive air systems. The structure of a heat pipe is shown in Figure 3.8. The flat copper envelope of the heat pipe was under partial vacuum. The capillary structure is made of sintered copper powder. The heat pipe uses water as the working fluid. Water on the evaporator side will absorb heat and become vapour lower 100 °C due to low pressure inside. Water on the condenser will dissipate heat to the surrounding and become liquid again. This cycle repeats again and again.

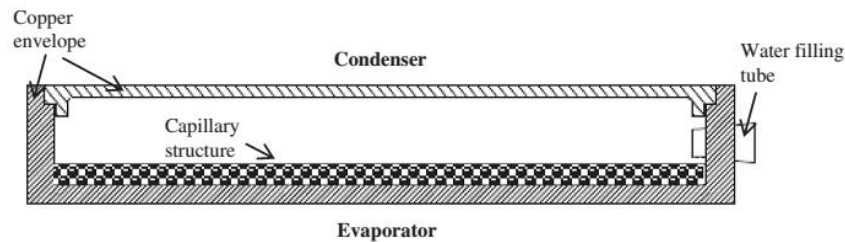


Figure 3.8 Structure of the heat pipe (Tran, 2014).

The following figure shows the schematic description of a heat pipe cooling system. A battery as heat source sits below the heat pipe (on the evaporating side). Cooling fins as heat sinks are on the heat pipe (on the condensing side). According to the conclusion of an experiment (Tran, 2014), heat pipe cooling system can reduce the thermal resistance by 30% under natural convection as compared to without heat pipe. A thermal resistance reduction of 20% under low air velocity convection is possible.

Note that, in comparison to thermo-electric, a heat pipe is more reliable, because there are no moving parts and no energy consumption. However, a heat pipe is unable to heat the battery due to its fixed structural layout.

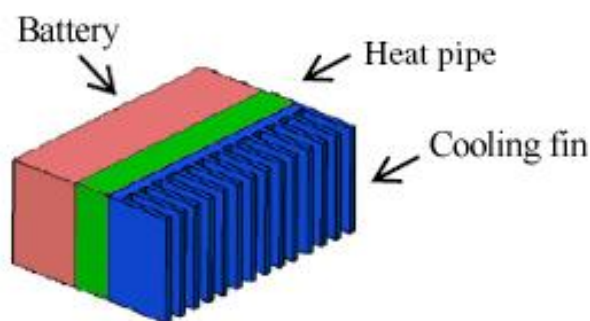


Figure 3.9 Scheme of heat pipe cooling system.

3.2.7 PTC Heater

PTC thermistors have many self-heated applications by utilizing their own voltage-current or current-time characteristics. One of the applications is as a self-regulating heater known as a PTC heater. The temperature of a PTC heater can be kept at a fixed point through adjusting the resistance of PTC heater automatically, see Figure 3.10. (Digikey, 2014)

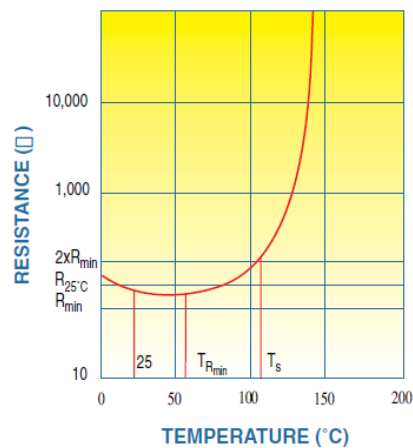


Figure 3.10 Resistance versus Temperature for a PTC (Digikey, 2014).

3.3 Evaluation of Different Technologies

Here the comparison of different battery thermal management systems has been made according to several items, see [Appendix A1](#).

3.3.1 Forced-Air System

Forced-air cooling system with a simple structure has the advantage of high reliability and low cost as well as easy maintenance, while it has poor thermal management, i.e. beyond operating temperature, uneven uniformity of temperature distribution and spread of thermal runaway.

In high ambient temperatures e.g. 45 °C-50 °C, the temperature inside the battery pack exceeds 55 °C which is beyond the operating temperature and will result in thermal runaway. The uniformity of temperature distribution is also crucial due to the effect of degradation and cycle life. If one ignores the ambient temperature, the difference between cells is 2 °C at the discharge current 2C-rate, and 4.8 °C at the discharge current 6.67C-rate. The uniformity of temperature distribution is also affected by the flow rate. As the flow rate increase, cell maximum temperature difference will increase, e.g. 3K at Re=136 and 4.8K at Re=1347. With the increasing flow rate, the cell maximum temperature difference can be even over 5K. (Sabbah, et al., 2008) It will give rise to degradation and the decrease of cycle life because the heat transfer between cells is quicker than the heat transfer from battery pack to air. So if one cell fails, thermal runaway will spread over the battery pack. (Kizilel, et al., 2009)

The following Table 3.1 shows that at the same flow rate the air volume is much bigger than the water volume, while the air heat transfer co-efficient is much lower than water heat co-efficient. So for air cooling to dissipate heat as much as water cooling, it requires higher volumetric flow rate which means more space and more power. Air

cooling system takes up larger space and consumes much more energy comparing to liquid cooling system.

Table 3.1 The volumetric flow rate and average heat transfer co-efficient at the same mass flow rate 50g/s (Pesaran, 2001).

	Volumetric flow rate(L/s)	Average heat transfer coefficient (W/m ² K)
Air	43	25
Mineral Oil	0.057	57
Water	0.049	390

3.3.2 Liquid System

There are three types of cooling systems, namely passive cooling system, active cooling system, and refrigerant cooling system.

The passive cooling system is affected by the ambient temperature, because the heat dissipation is dependent on the radiator and the radiator dissipates heat through the temperature difference between liquid and the ambient temperature. Under normal circumstances, it works well, but under high ambient temperature it is insufficient.

Active cooling systems have good thermal performance which can keep the battery pack within the operating temperature and keep temperature distribution between cells even because of high heat co-efficient of the coolant. Due to many auxiliaries and moving parts, the structure is complicated and difficult to maintain. It also has the tendency of leaking out.

Compared to active cooling systems, direct refrigerant cooling systems are more efficient because they use refrigerant directly to cool the system instead of using refrigerant to cool coolant first and then using coolant to cool the system. The weaknesses of refrigerant cooling system are complicated structure and difficult maintenance, as well as potential to leak out and so on.

3.3.3 PCM System

PCM cooling systems perform well on thermal management. Even under high ambient temperatures from 45 °C to 50 °C, the temperature inside the cell pack is always below 55 °C because of high thermal conductivity and latent heat. (Sabbah, et al., 2008) Table 3.2 shows the characteristics of PCMs. In the case of stressful situations e.g. at current discharge rate 6.67C-rate and ambient temperatures of 45 °C, the cell maximum temperature difference doesn't exceed 0.5K. And at normal conditions the difference of temperature between cells is negligible. (Sabbah, et al., 2008) If one cell fails, thermal runaway will not propagate because the PCM-graphite matrix absorbs and spreads the heat quickly. (Kizilel, et al., 2009)

The weakness of PCM is that it is more suitable for cold conditions or in space. When the temperature of the battery pack is higher than the temperature of the PCM melting

point, heat is stored as latent heat and will be released to the module of battery when the ambient temperature is lower than the temperature of the PCM melting point.

The structure of PCM without new components is simple, light and space-saving. But it still has the potential of flammability and electrical conductivity as well as volume change due to the characteristic of the PCM-graphite.

Table 3.2 The thermal characteristics of PCM.

	Density(g/cm ³)	Latent heat(J/g)	Heat conductivity(W/(m K))
PCM(L)	0.79	173.6/266	0.167
PCM(S)	0.916		0.346

3.3.4 Thermo-electrics

Thermo-electrics have small and lightweight structures and can turn a heating element to an efficient cooling element by reversing the polarity. Without moving parts to wear, thermo-electrics are reliable, durable and of low maintenance. And also easy to replace in case of failure. In addition, operation is quiet and vibration-free. (Binder, 2014)

The weakness of thermo-electrics is low efficiency. The highest efficiency is up to 0.8 which means more power is needed than heat dissipated. (Huairui, 2014)The performance is associated with the required temperature difference. The greater the temperature difference is, the lower the pumping capacity is, until it stops working at 70K. So under high temperature the temperature difference is great and thermo-electrics perform badly. And there is one technical problem not solved: that the hot and cold sides are close to each other. (Binder, 2014)

3.4 Recommended Cooling System

Through the trade-off of the items mentioned above, two cooling systems are recommended, see [Appendix A3](#).

As seen in [Appendix A2](#), the performance of the items is described as a score and the importance of the items is described as a weighting factor. The product of score and weighting factor is the total score of the system, see [Appendix A3](#). The systems of the two highest scores are the recommended systems.

3.4.1 Combined Liquid System (CLS)

The first is the liquid cooling system, which has four working modes: bypass with heater working; bypass without heater working; passive cooling system; and active cooling system (see Figure 3.11). The cooling system takes advantage of both passive cooling system and active cooling system. Passive cooling system has simple structure and is able to dissipate heat under normal conditions with low energy consumption. Under extreme condition, active cooling system has good thermal performance to keep battery temperature in the required range.

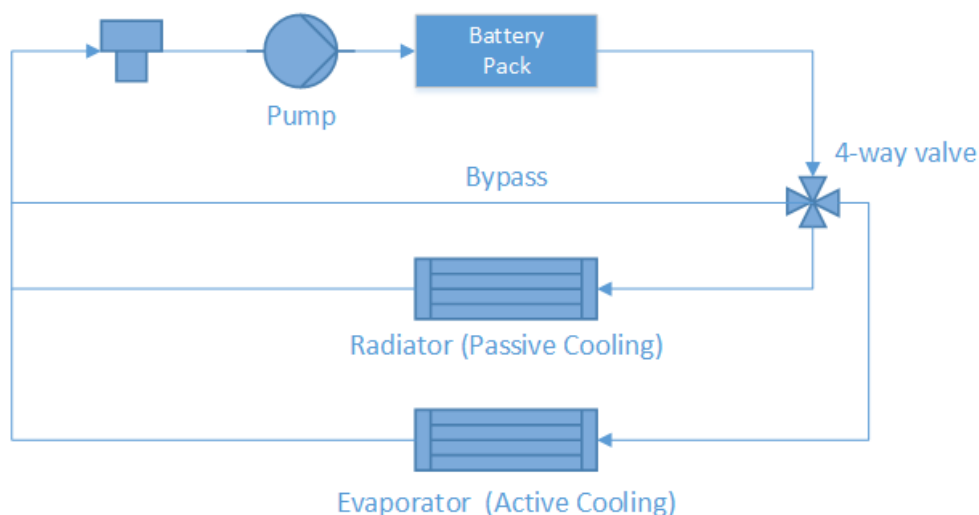


Figure 3.11 The combined liquid system.

3.4.2 PCM Model (CLS+PCM)

The other preferred system is the combination of PCM material and CLS. PCM layers are inserted into battery pack. It uses the advantage of PCM to have good thermal performance, and CLS compensates for the limited operating temperature of PCM, see Figure 3.12.

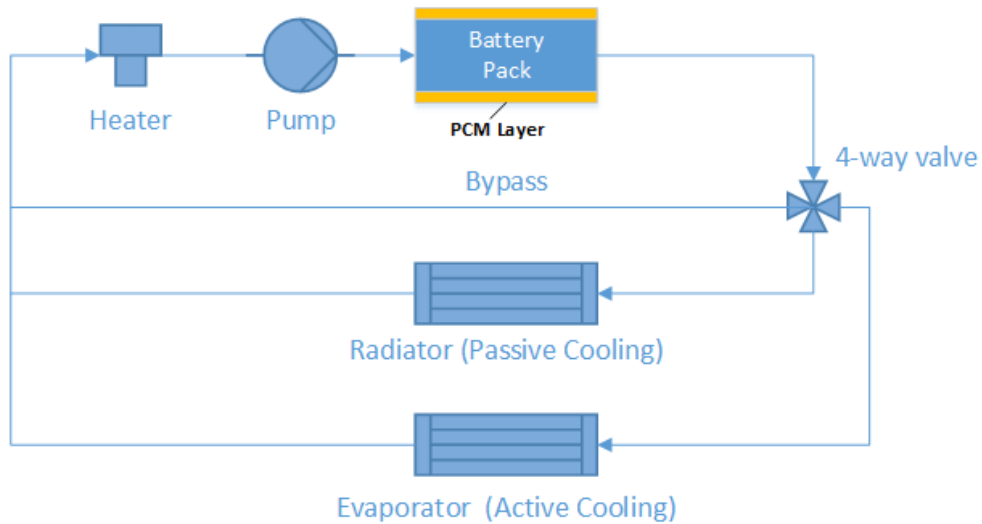


Figure 3.12 The combined liquid system with PCM system

4 Modelling of BTMS

Before starting to build up a MATLAB/Simulink model, a logic model was built to construct an overall logic framework of BTMS simulation. It helped not only with the following steps of modelling but also the possibility of future modification, extension and improvement. A detailed graphic description is shown in [Appendix B1](#).

The logic modelling was developed mainly in four steps:

- **Initial inputs and thermal cycles settings**
Starting with the battery unit, physical parameters such as thermal capacity and mass were defined as fixed parameters. When the PCM is located close to the battery cell, these two parts could be treated as one integrated part. Thus the PCM in this case could be considered a part within the battery unit. Focusing on the thermal issues of the battery pack, there are two main parts of heat transfer flows that influenced the battery temperature. One was the heat generation internally. This part depended on driving behaviour, battery features and other vehicle parameters, such as vehicle mass and aerodynamic performance. Since this thesis focused on thermal rather than electro-thermal issues, this interior heat was generated by exterior electro-thermal model. The other part was the external heat dissipation. This part of the heat was from the different thermal cycles which took away certain amounts of heat from the battery or in some cases brought heat to the battery. The amount of heat depended both on which thermal cycle was chosen and surrounding thermal conditions. Therefore, some parameters were collected from the battery unit and testing conditions for calculation. After this step the required battery thermal model was built.
- **Control strategy development**
Normally, there are more than two thermal cycles designed in battery thermal models. To decide which cycle to operate, some characteristic parameters were required, such as battery temperature and ambient temperature. According to these parameters, an operation state was chosen. The state corresponding to the thermal cycle that was active and some related components, for example, the pump would change their operating state as well. In some cases a sub-state under the main operation state could be introduced in order to achieve better operation feature.
- **Simplification and decoupling**
Some complex calculation cases would give endless loops thus a simplified or approximate calculation method should be adopted to solve the endless loops and to accelerate the simulation. In other cases, decoupling was an alternative solution. For example, the activated thermal cycle consumes electricity, causing additional load and consequently additional heat. This coupling between the thermal model and electro-thermal model would cause unexpected programming issues. Thus, it was better to decouple these two models at the beginning and connect them later when both of them worked well.
- **Data process and output**
Not all output parameters were meaningful. Only parameters which represented the outcome of the model were recorded. Some raw data was processed into performance parameters (see Section 4.4) in order to evaluate different results with a common standard. For a better visual understanding, some figures were also plotted based on numerical data.

4.1 Modelling Conditions

Both of the models were built up based on almost the same conditions, meaning that most parameters were the same. Some important ones are listed in the following Table 4.1.

Table 4.1 Some important fixed modelling parameters.

Parameter	Value	Comment
Battery capacity	29.5 kWh (17.7 kWh available)	60% available capacity, SOC=20% - 80%
Battery mass m_{ba}	270 kg	-
Battery specific heat capacity $C_{p,ba}$	1000 J/kg K	-
Vehicle mass m_{veh}	1700kg	passengers included

Also, a few parameters varied in order to represent different situations. The most important variable parameters were:

- Ambient temperature T_{amb}
This temperature represented the climate conditions of the atmosphere around the driving vehicle. When it ranged from -20 °C to 10 °C, it was considered to be a cold climate. When it ranged from 10 °C to 20 °C, it was considered to be a mild climate. When it ranged from 20 °C to 40 °C, it was considered to be a hot climate.
- Battery initial temperature $T_{ba,ini}$
It's normally considered that battery initial temperature is exactly equal to ambient temperature. But when pre-conditioning is applied, these two temperatures are not the same. Battery initial temperature is higher than ambient temperature when the battery is pre-heated in a cold climate. Battery initial temperature is lower than ambient temperature when the battery is pre-cooled in a hot climate. Different levels of pre-conditioning could be adopted.
- Desired temperature T_{des}
The desired temperature represents the temperature that the control unit of the BTMS aims for, i.e. the optimum operating temperature point stated by the manufacturer. With different thermal cycles the BTMS will try to control battery temperature as close as possible to the desired temperature. In most cases of this work T_{des} is 25 °C, but some special cases with $T_{des} = 20$ °C were also tested.
- Testing driving cycle **TDC**
As mentioned in [Section 1.3 Limitation](#), this model focuses more on the BTMS feature during driving. Two **driving cycles** were chosen to represent two different driving behaviours: One was US06 whose vehicle speed profile is shown in Figure 4.1. This driving cycle lasts 596 seconds per single cycle. It has an aggressive driving behaviour with maximal speed of 129 kph and an average speed of 77.9 kph. The other is the NEDC (New European Driving Cycle) representing a mild driving behaviour (see Figure 4.2). It lasts 1180 seconds per

single cycle with maximal speed of 120 kph and an average speed of 33.9 kph. For testing, each was chosen as a testing condition input and the vehicle was driven following the speed profile until the available battery capacity (17.7 kWh) was exhausted. This complete cycle is called **Testing Driving Cycle (TDC)** which consisted of several driving cycles. The whole TDC NEDC lasted 16229 seconds and TDC US06 5139 seconds.

According to the different TDC, the corresponding heat generation rate profile was calculated through exterior electro-thermal model and the profile of the NEDC is shown in Figure 4.3. Another heat generation rate profile by US06 was generated in the same way.

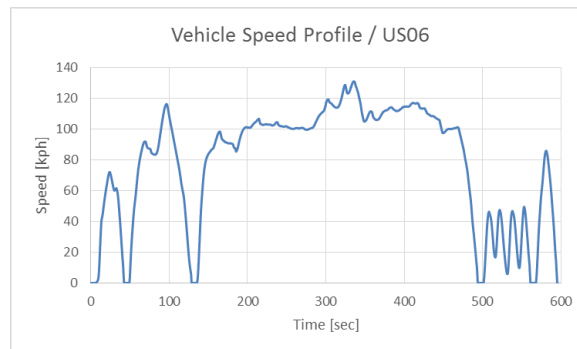


Figure 4.1 Vehicle speed profile of driving cycle US06.

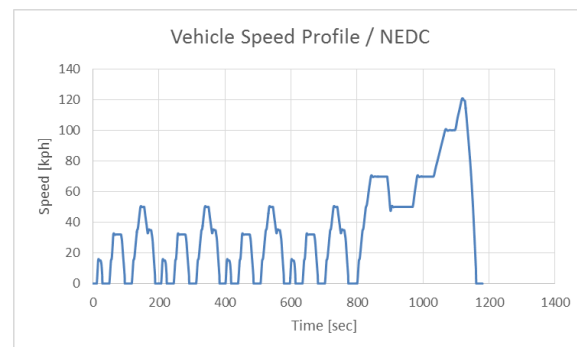


Figure 4.2 Vehicle speed profile of driving cycle NEDC.

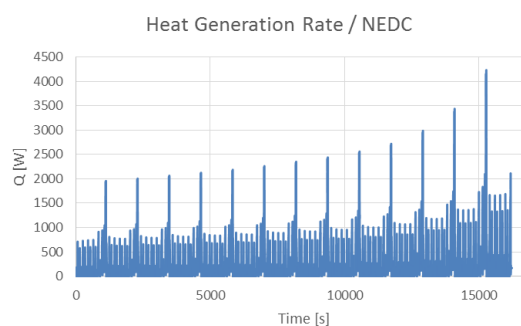


Figure 4.3 Heat generation rate profile of NEDC.

4.2 CLS Model

Based on the system layout of CLS in Section 3.4.1, a MATLAB/Simulink model was developed following the four steps mentioned at the beginning of this chapter.

A basic model layout is shown in the following Figure 4.4. The complete model layout is attached in [Appendix B2](#).

In the basic layout, the temperature flow of heat transfer fluid connects the main parts together. In initial step, testing data was loaded. Then starting with the battery unit the fluid was heated up. Afterwards, the fluid flows through different parts, but only one outcome was chosen by control unit. The flow rate of the pump was also governed by control unit. Lastly, the coolant returned to battery pack. This calculation process was repeated until the driving cycle ended.

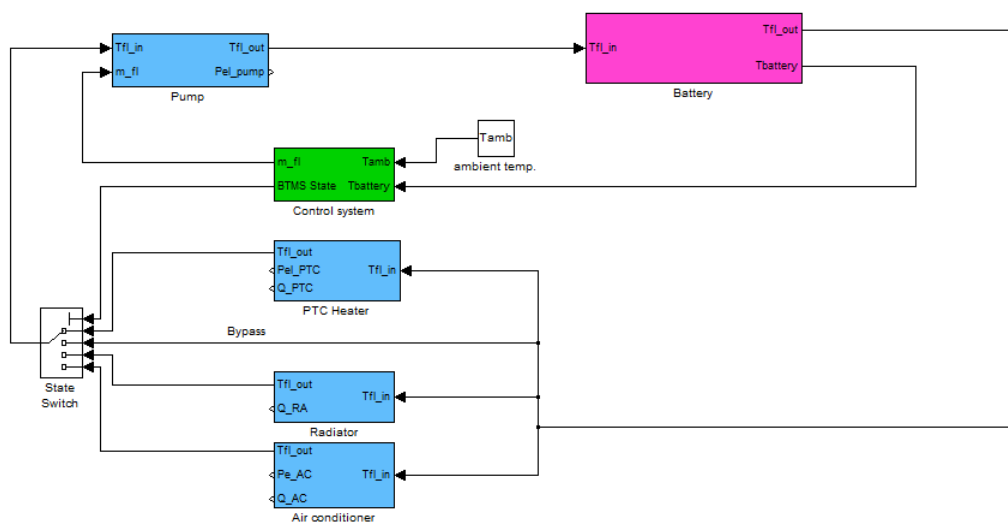


Figure 4.4 Basic Simulink model layout for CLS.

4.2.1 Battery Unit

It was assumed that the parts of battery cells were homogeneous and the interior heat conductivity between cells approaches infinity so that the heat transferred between cells very quickly and that all points on the battery cells had the same temperature, called battery temperature T_{ba} . The differential of battery temperature over time is stated with the following equation:

$$\frac{dT_{ba}}{dt} = \frac{\dot{Q}_{gen} - \dot{Q}_{dis}}{m_{ba}c_{p,ba}} \quad (4.1)$$

\dot{Q}_{gen} and \dot{Q}_{dis} states respectively heat generation rate and heat dissipation rate. The former is set up by the program interior signal generator or by heat generation rate profile of either US06 or NEDC (see Figure 4.3). This heat represents the heat generated through battery electro-thermal effects. The later one was calculated by sub-system of the battery unit, which is expressed in Equation 4.2. This heat represents the heat dissipated through thermal cycle(s). The value is positive when thermal cycle is in

cooling operation. The value is negative when thermal cycle is in heating operation. m_{ba} and $C_{p,ba}$ is battery mass and specific heat capacity of battery

$$\dot{Q}_{dis} = UA(\overline{T}_{fl} - T_{ba}) \quad (4.2)$$

In the battery pack, three discrete copper tubes are jointed very closely to the battery cells in order to transfer heat to and from the battery. Overall heat transfer co-efficient U will be thus calculated as mentioned in Section 2.2.1. A represents the contact area which is the total inner area of the three tubes. $\overline{T}_{fl} - T_{ba}$ represents the approximate mean temperature difference. \overline{T}_{fl} is the mean temperature of fluid inlet and outlet temperature.

4.2.2 Air Conditioner (Active Cooling)

When heat transfer fluid flows through air conditioner, the fluid temperature differential is expressed as the following equation varied from Equation 2.12:

$$\frac{dT_o}{dt} = \frac{\dot{m}_{fl}C_{p,fl}(T_i - T_o) - \dot{Q}_{AC}}{m_{fl,AC}C_{p,fl}} \quad (4.3)$$

The air conditioner always takes heat from the fluid, thus \dot{q} in Equation 2.12 is always negative. Here \dot{q} is replaced by $-\dot{Q}_{AC}$ where \dot{Q}_{AC} means cooling load of air condition and is always positive. \dot{Q}_{AC} can be calculated by the following equation:

$$\dot{Q}_{AC} = P_{el,AC} \cdot COP \quad (4.4)$$

$P_{el,AC}$ is the electricity consumption by air conditioner and COP is Co-efficient of Performance which is dependent on working condition of air conditioner.

4.2.3 Radiator (Passive Cooling)

Similar to the air conditioner, the fluid temperature differential in the radiator can be expressed as:

$$\frac{dT_o}{dt} = \frac{\dot{m}_{fl}C_{p,fl}(T_i - T_o) - \dot{Q}_{RA}}{m_{fl,RA}C_{p,fl}} \quad (4.5)$$

Where \dot{Q}_{RA} is the product of overall heat transfer co-efficient, contact area and temperature difference of inlet fluid temperature and ambient temperature:

$$\dot{Q}_{RA} = UA(T_{fl,in} - T_{amb}) \quad (4.6)$$

and the product UA is given by the technical performance maps of the chosen radiator. It is expressed as a function of fluid mass flow rate and air flow rate:

$$UA = f(\dot{m}_{fl}, \dot{m}_{air}) \quad (4.7)$$

In other expression, \dot{Q}_{RA} is decided by temperature difference between fluid and ambient, fluid mass flow rate and air flow rate these three terms:

$$\dot{Q}_{RA} = f(\dot{m}_{fl}, \dot{m}_{air}, T_{fl,in} - T_{amb})$$

4.2.4 PTC Heater (Heating)

Heater energy balance equation is expressed as:

$$mC_p \frac{dT_{out}}{dt} = \dot{m}C_p(T_{in} - T_{out}) + \dot{Q} \quad (4.8)$$

where \dot{Q} is the heat provided by heater, T_{in}, T_{out} is the temperature of coolant in and out, \dot{m} is the coolant mass flow rate, m is the coolant mass in tubes.

PTC heater is widely used as an electrical vehicle heater and it has two main characteristics (Lauda, 2014):

$$P = P_{max} = const \quad (4.9)$$

$$m_{fl} = m_{fl, rated} \quad (4.10)$$

Where the heater power P is always equal to the maximum heater power P_{max} , the mass of flow rate m_{fl} is constant.

4.2.5 Pump

The electrical energy consumption of the pump is expressed as the following:

$$P = \frac{YH\dot{m}}{\eta} \quad (4.11)$$

where the specific gravity Y is the multiplication of the coolant density and gravity and expressed as:

$$Y = \rho g \quad (4.12)$$

where \dot{m} is the mass flow rate, η is the efficiency of the pump, H is the total head and is related to the mass flow rate \dot{m} , see Figure 4.6:

$$H = f(\dot{m}) \quad (4.13)$$

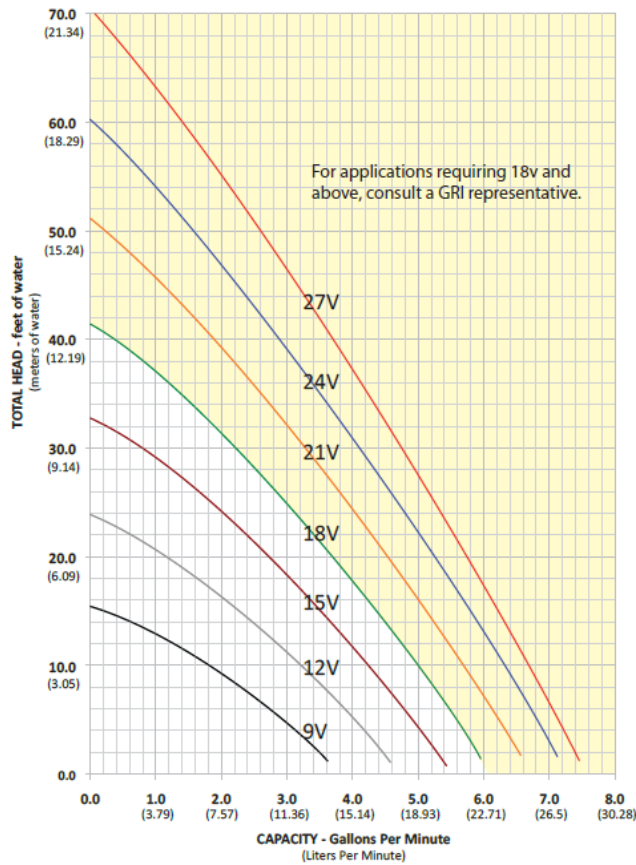


Figure 4.5 The relationship between flow rate and total head (Gripumps, 2014).

The Figure 4.6 shows the water pump performance and for other viscous coolant the correction is used to determine the performance (Mc Nally Institute, 2014):

$$\dot{m}_{cl} = C_p \dot{m}_w \quad (4.14)$$

$$H_{cl} = C_h H_w \quad (4.15)$$

$$\eta_{cl} = C_\eta \eta_w \quad (4.16)$$

where C_p , C_h , C_η are capacity correction factor, head correction factor and efficiency correction factor respectively. Due to the low viscosity and similarity to water of the coolant, the correction factors are chosen as:

$$C_p, C_h, C_\eta = 1 \quad (4.17)$$

4.2.6 Control Unit

Generally, a complex on-off control strategy is applied which has already been introduced in Section 2.3. Here three on-off controllers with different switching temperatures create four states and each state matches an operation modus. Controller I controls the switching between State 1(Heating) and State 2(Bypass). Controller II controls the switching between State 2 and State 3(Passive cooling). Controller III controls the switching between State 3 and State 4(Active cooling).

Table 4.2 Switching points of three on-off controllers ($T_{des}=20/25\text{ }^{\circ}\text{C}$).

On-off controller	Lower switching temperature	Upper switching temperature	State	Operation
I	-	10	1	Heating
			2	Bypass
II	$T_{des} - 2$ (18/23 $^{\circ}\text{C}$)	T_{des} (20/25 $^{\circ}\text{C}$)	3	Passive Cooling
III	T_{des} (20/25 $^{\circ}\text{C}$)	$T_{des} + 2$ (22/27 $^{\circ}\text{C}$)	4	Active Cooling

Note that, for controller I, there is no lower switching temperature or the lower switching temperature is the same as the upper switching temperature of 10 $^{\circ}\text{C}$. The reason to set up this on-off controller is to heat the battery with the PTC heater when the battery is below the lower temperature limit of 10 $^{\circ}\text{C}$ (Section 2.1.3) and to switch the state into 2 (Bypass) when battery is heated up above 10 $^{\circ}\text{C}$. Since the focus is the driving cycle and the cooling load from ambient is negligible, the battery temperature will not drop below 10 $^{\circ}\text{C}$ again after it has been above 10 $^{\circ}\text{C}$. Thus, the lower switching temperature is invalid here. For controller II and III, variable switching points are introduced in order to create a flexible control strategy. However, T_{des} is set to 25 $^{\circ}\text{C}$ in most cases. Only in a few cases T_{des} was set to 20 $^{\circ}\text{C}$.

Besides the basic strategy described above, there are two improvements for better performance:

1. Forced switching to active cooling

There is one exceptional situation which the control unit has to face. It is that the ambient temperature is higher than desired temperature. In this case the passive cooling is invalid and even has a negative effort i.e. bringing heat to the battery. Thus, the state of passive cooling should be forced to switch to active cooling when ambient temperature is higher than $T_{des} - 4\text{K}$. The reason to set this temperature point is that the radiator operates when battery temperature is from T_{des} until to $T_{des} - 2\text{K}$. To make passive cooling efficient, a temperature difference between the battery and ambient temperature of an extra 2K is needed. Thus, the ambient temperature should be lower than $T_{des} - 4\text{K}$ ($T_{des} - 2\text{K} - 2\text{K}$) to make sure that passive cooling works properly and efficiently. The control strategy for this is shown in Table 4.3.

2. Sub-states during active cooling

Another improvement of control unit is achieved by dividing active cooling into three sub-levels. The higher the battery temperature, the more powerful the active cooling is. The switching points of the controller are shown in Table 4.4. With this improvement, electricity could be further saved when battery temperature is low and cooling is not so urgently required. Moreover, a high AC level offers more powerful cooling and ensures safety during high battery temperature.

Table 4.3 Control strategy for the high ambient temperature ($T_{des}=20/25\text{ }^{\circ}\text{C}$).

Lower switching temperature	Upper switching temperature	State	Operation
-	10	1	Heating
$T_{des} - 2$ (18/23 $^{\circ}\text{C}$)	T_{des} (20/25 $^{\circ}\text{C}$)	2	Bypass
		4	Passive Cooling

Table 4.4 Sub-states of active cooling ($T_{des}=20/25\text{ }^{\circ}\text{C}$).

Lower switching temperature	Upper switching temperature	State	Operation
$T_{des} + 1$ (21/26 $^{\circ}\text{C}$)	$T_{des} + 3$ (23/28 $^{\circ}\text{C}$)	4.1	AC level low
$T_{des} + 2$ (22/27 $^{\circ}\text{C}$)	$T_{des} + 4$ (24/29 $^{\circ}\text{C}$)	4.2	AC level medium
		4.3	AC level high

4.3 PCM Model

To verify the usage and effectiveness of PCM, the PCM unit is inserted into the battery pack of the liquid cooling system.

The state of the PCM is controlled by the battery temperature and heat generated by battery, see Figure 4.7.

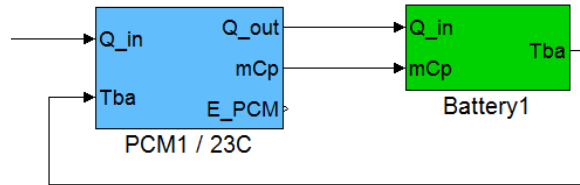


Figure 4.6 PCM unit with battery in battery pack.

The model is simplified and the temperature of the PCM is equal to the battery temperature ignoring the process of melting and solidifying:

$$T_{PCM} = T_{ba} \quad (4.18)$$

The battery temperature is defined as:

$$\frac{dT_{ba,PCM}}{dt} = \frac{\dot{Q}_{gen} - \dot{Q}_{dis} - \dot{Q}_{absorbed}}{m_{ba}C_{p,ba} + m_{PCM}C_{p,PCM}} \quad (4.19)$$

Where \dot{Q}_{gen} is the heat generated by the battery, \dot{Q}_{dis} is the heat dissipated by the cooling system, $\dot{Q}_{absorbed}$ is the heat absorbed and stored by the PCM as latent heat.

The point at which the PCM starts to store heat depends on the battery temperature. If battery temperature exceeds the melting temperature of the PCM, heat will be absorbed by the PCM and stored as latent heat at a certain temperature. When battery temperature goes below the melting temperature, the latent heat will be released.

Table 4.5 An illustrative table for PCM unit.

Battery Temperature	PCM Latent heat
$T_{battery} < T_{melting}$	$Q_{absorbed} = 0$
$T_{battery} = T_{melting}$ $Q_{gene} < H_{max}$	$Q_{absorbed} = Q_{gene}$
$T_{battery} > T_{melting}$ $Q_{gene} > H_{max}$	$Q_{absorbed} = H_{max}$

where H_{max} is the total latent heat of PCM.

The PCM melting temperature is set to 23 °C. During driving, the latent heat stored in the PCM will not be released and instead it will be dissipated by BTMS.

4.4 Performance Parameters

In the following, the equations of performance parameters are briefly shown. It includes the electrical energy consumption of each component and the temperature of the battery as well as the working time for each component.

The total electrical energy consumption is formulated as a combination of electrical energy consumed by each component:

$$E_T = \sum E_{HT} + E_{BP} + E_{PC} + E_{AC} \quad (4.20)$$

The heater consumption is obtained through the integration of heater power and pump power when the heater works:

$$E_{HT} = \int P_{PTC} + P_{pump} dt \quad (4.20)$$

The bypass consumption is calculated by the integration of pump power when the coolant is going through the bypass:

$$E_{BP} = \int P_{pump} dt \quad (4.21)$$

The air conditioner consumption is the sum of the integration of air condition power and pump power when the air conditioner works:

$$E_{AC} = \int P_{AC} + P_{pump} dt \quad (4.22)$$

The maximum battery temperature is defined as:

$$T_{b,max} = \max T_b(t) \quad (4.23)$$

The average battery temperature is calculated as:

$$T_{b,ave} = \overline{T_b(t)} \quad (4.24)$$

The average battery temperature $T_{b,ave,c}$ represents the average battery temperature during passive cooling and active cooling. It is characterized by the following equation:

$$T_{b,ave,c} = \overline{T_b(t1)} \quad (4.25)$$

In addition, there are some other parameters to evaluate the model performance.

t_{HT} , t_{BP} , t_{PC} and t_{AC} represent operating duration of heating, by-pass, passive cooling and active cooling respectively.

t_{10} is the time when the battery temperature is above 10 °C for the first time after driving cycle starts at cold condition.

t_{des} is expressed as the time when the battery temperature is below the desired temperature for the first time after driving cycle starts at hot condition.

t_{PCM} (PCM only) is to evaluate how long the PCM can keep the battery at the melting temperature by using latent heat.

5 Results and Discussion

In following sections, two models are tested under different conditions which are described in Section 4.1. In addition, for the PCM model the mass of the PCM will affect the energy consumption. Thus, a detailed comparison between the PCM model and the CLS model is included.

5.1 CLS Model

For better visual understanding of the modelling results, four types of figures are generated by Simulink with numerical result. They show temperature, energy consumption, transferred heat and overview in detail. An example is introduced for the condition NEDC, $T_{amb}=20\text{ }^{\circ}\text{C}$, $T_{ba_ini}=20\text{ }^{\circ}\text{C}$ and $T_{des}=25\text{ }^{\circ}\text{C}$. More details are attached in [Appendix C](#).

Figure 5.1 shows the temperature changes over time. Blue curve represents the battery temperature; green, the heat transfer fluid (coolant) inlet temperature before battery unit; and red, the coolant outlet temperature after battery unit.

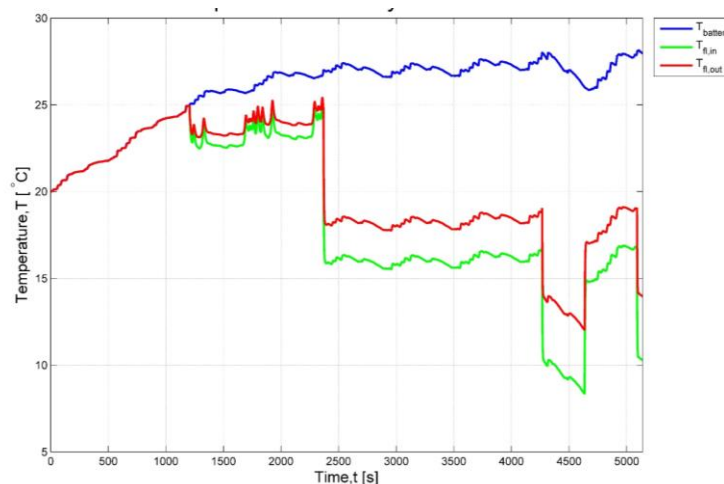


Figure 5.1 Temperature feature of battery and coolant over time.

Figure 5.2 summarizes the electricity consumption of different components and also the total. Note that, for passive cooling, the radiator consumes nothing by itself and only pump energy consumption has been taken into account.

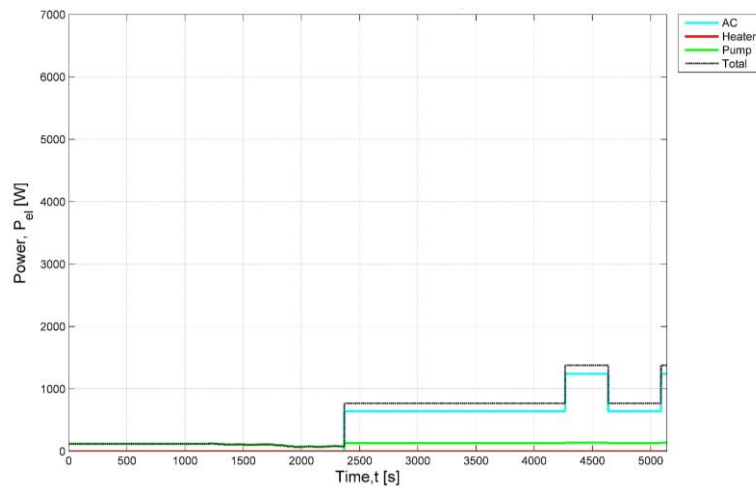


Figure 5.2 Electricity consumption feature.

Figure 5.3 shows the heat transferred between fluid and battery. Red curve is for heating (in this result equal to zero); cyan is for passive cooling; and blue is for active cooling. In this figure, the effective cooling or heating power of the battery is shown in detail.

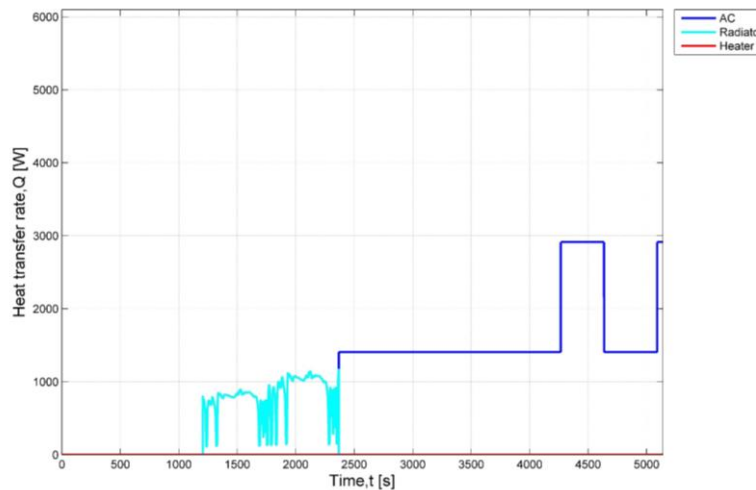


Figure 5.3 Heat transfer feature.

Figure 5.4 gives an overview of the whole operation feature. It consists of information about heat generation rate, battery temperature, state of the BTMS and pump flow rate.

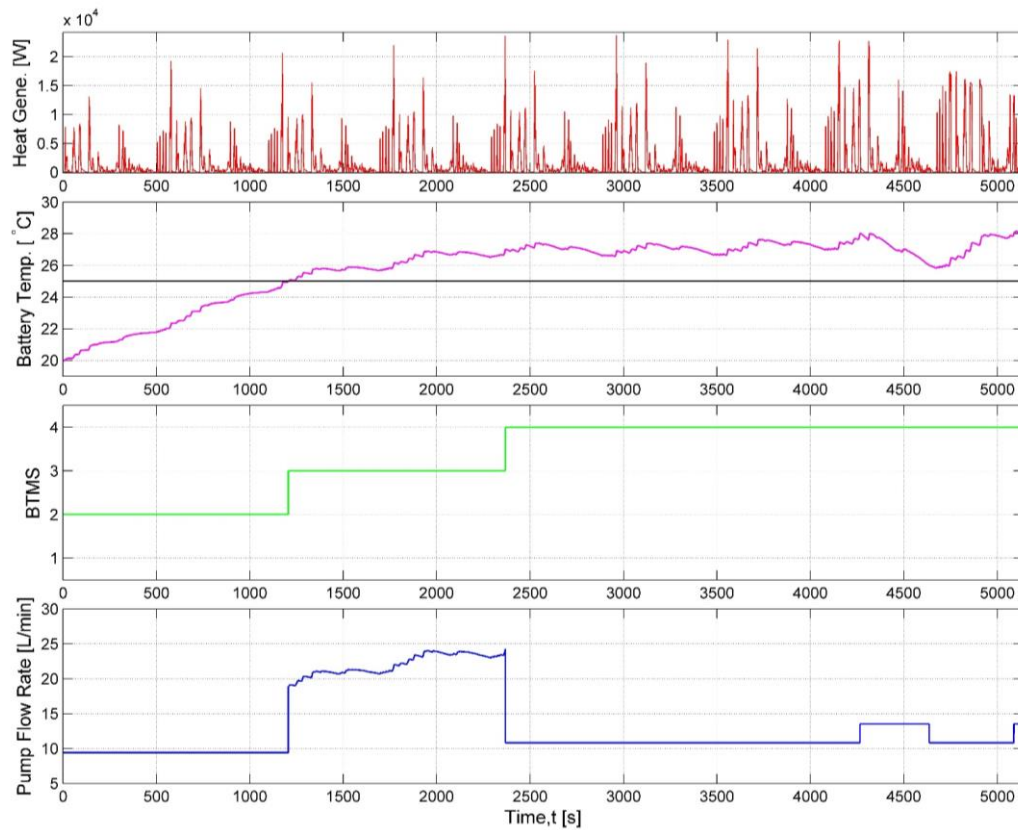


Figure 5.4 Overview operation feature.

5.1.1 NEDC versus US06

Customers drive their cars in different ways. Thus, two driving cycles representing two styles are tested with these models. The ambient temperature varied from -20 °C to 40 °C with an interval of 10 °C. The battery initial temperature was equal to the ambient temperature i.e. there was no pre-conditioning introduced. The following diagrams show a comparison of energy consumption between the two driving cycles. The different colors show accumulated electricity consumption of different BMTS states for the whole TDC. Also, the table below the diagram shows the exact sub-total, the total electricity consumption and its percentage in available battery capacity.

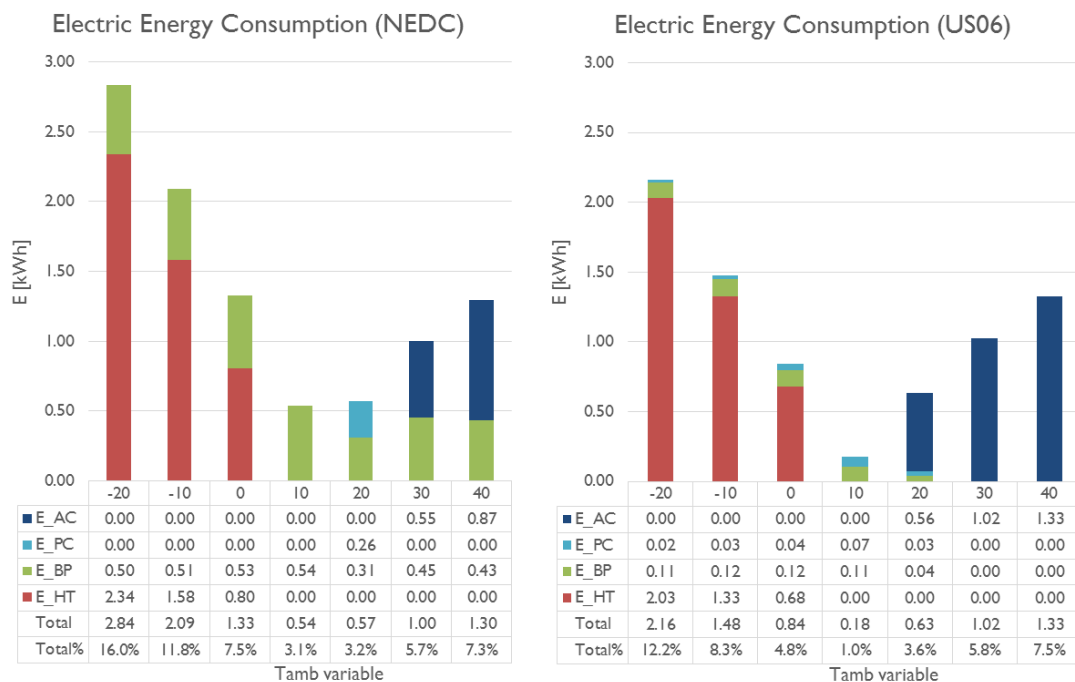


Figure 5.5 Electricity Consumption for TDC NEDC and US06.

There are several points to be highlighted:

- In cold and hot weather, more electricity is used. Both diagrams show the tendency that the colder or hotter the weather is, the more energy will be used. Especially in extreme weather, the total soon rises. The electricity required for the NEDC accounted for 16% of total available battery capacity at the ambient temperature of -20 °C. It therefore shortened the electric range significantly.
- NEDC consumed more in cold weather and less in hot weather. US06 was the opposite. US06, as an aggressive cycle, had a higher heat loss, thus generating more heat during driving. Consequently, it utilized the heat generated by itself for heating in cold weather and less electricity for heating was required. Conversely, in hot weather, due to high heat generation rate, much more cooling load was needed. Therefore, TDC US06 consumed more electricity than NEDC.

- In mild weather pump consumption dominates
To compare both results at an ambient temperature of 10 °C, the pump consumed more with the TDC NEDC. The reason for this was the NEDC lasted 16229 seconds which was about three times longer than US06 and the energy used during bypass state (only pump operating) dominated the total.

5.1.2 Cold and Hot Weather

From Figure 5.5 it is obviously concluded that electricity consumption by BTMS is much higher in cold and hot weather than it is in mild weather. Optimization is required. One method to save energy would be to increase battery initial temperature in advance. In other words, the battery should be kept close to the operation temperature range as much as possible. This improvement could be realized by better insulation or/and active pre-conditioning. Here active pre-conditioning was further investigated as a potential energy saving measure. Active pre-conditioning means that the battery will be heated up in cold weather (pre-heating) or be cooled down in hot weather (pre-cooling) **before** driving. Its advantage is to prepare the battery in the operating temperature range in advance and thus the battery can work optimally with full performance. In addition, if the battery charger is connected, pre-conditioning makes use of electricity from power grid instead of consuming battery capacity, i.e. it can save energy and offers longer electric range of EV.

The following figure shows how much contribution pre-heating can make. The ambient temperature was fixed at -20 °C. The battery initial temperature (T_{ba_ini}) varied from -20 °C (meaning no pre-heating) via -10 °C and 0 °C up to 10 °C. It was assumed here that the EV was connected to the power grid and thus the energy consumed by pre-conditioning was not taken into account in the energy consumption for testing driving cycle. From this figure it will be seen that the pre-heating reduces electricity consumption dramatically. The maximum saving potential could reach 91% when the battery was heated to 10 °C in advance.

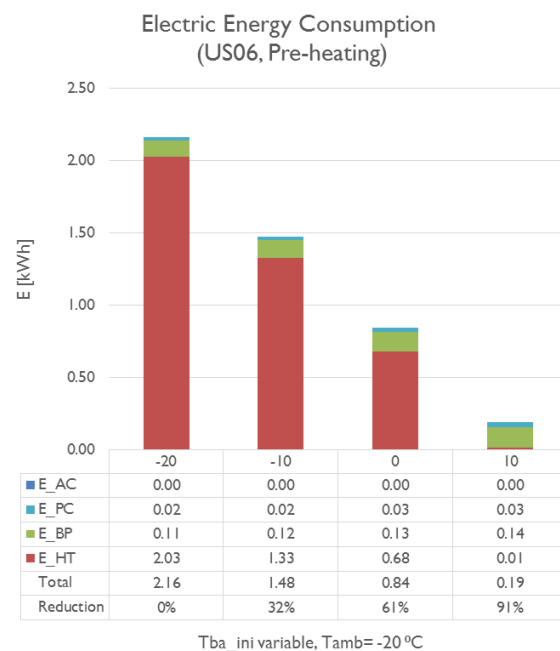


Figure 5.6 Energy saving by pre-heating for US06.

Another probable issue of BTMS in cold weather is passive cooling. The figure 5.7 shows the temperature changes of the battery and coolant. Around 4100 seconds and the 4600 seconds, there were two intervals for passive cooling. The inlet fluid temperature fell below 0 °C and the temperature difference between fluid and battery was larger than 20K. This large temperature gradient would potentially damage battery lifetime. This issue was caused by too high a pump flow rate which consequently resulted in too high cooling power. A special control of the pump could be introduced in future work for passive cooling in cold weather in order to reduce pump flow rate and to offer coolant of proper temperature.

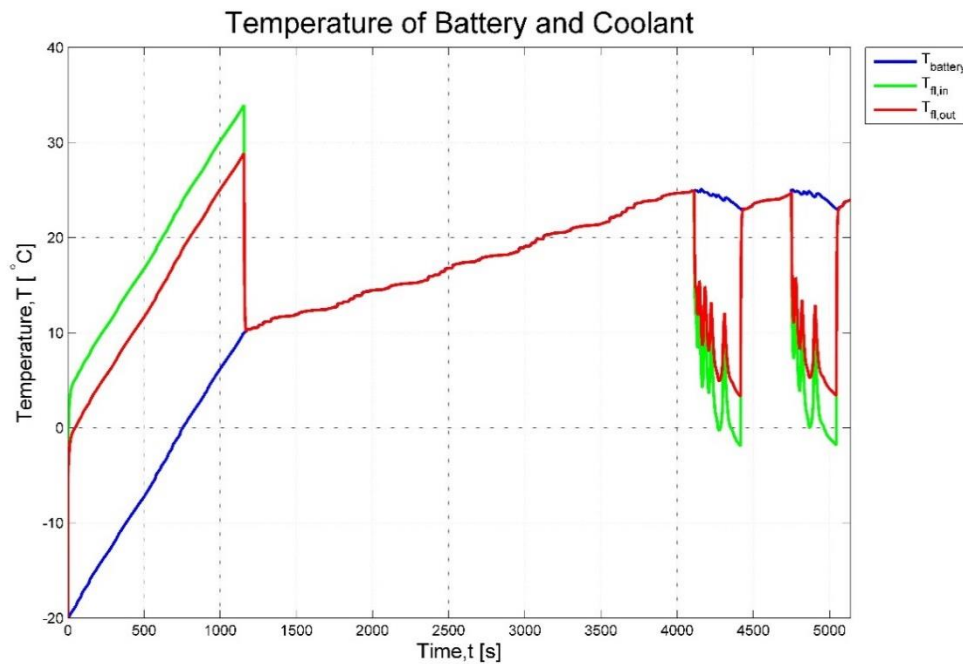


Figure 5.7 Temperature feature for US06, $T_{amb} = -20$ °C.

Similar to cold weather, electricity consumption in hot weather could be further saved by pre-cooling. Figure 5.8 shows the results for testing driving cycle US06 with fixed ambient temperature of 30 °C and variable battery initial temperature from 30 °C (means no pre-cooling) via 25/20/15 °C to 10 °C. The reduction of electricity consumption was not as significant as that by pre-heating, but there was still about half saved when the battery was cold down to 10 °C in advance.

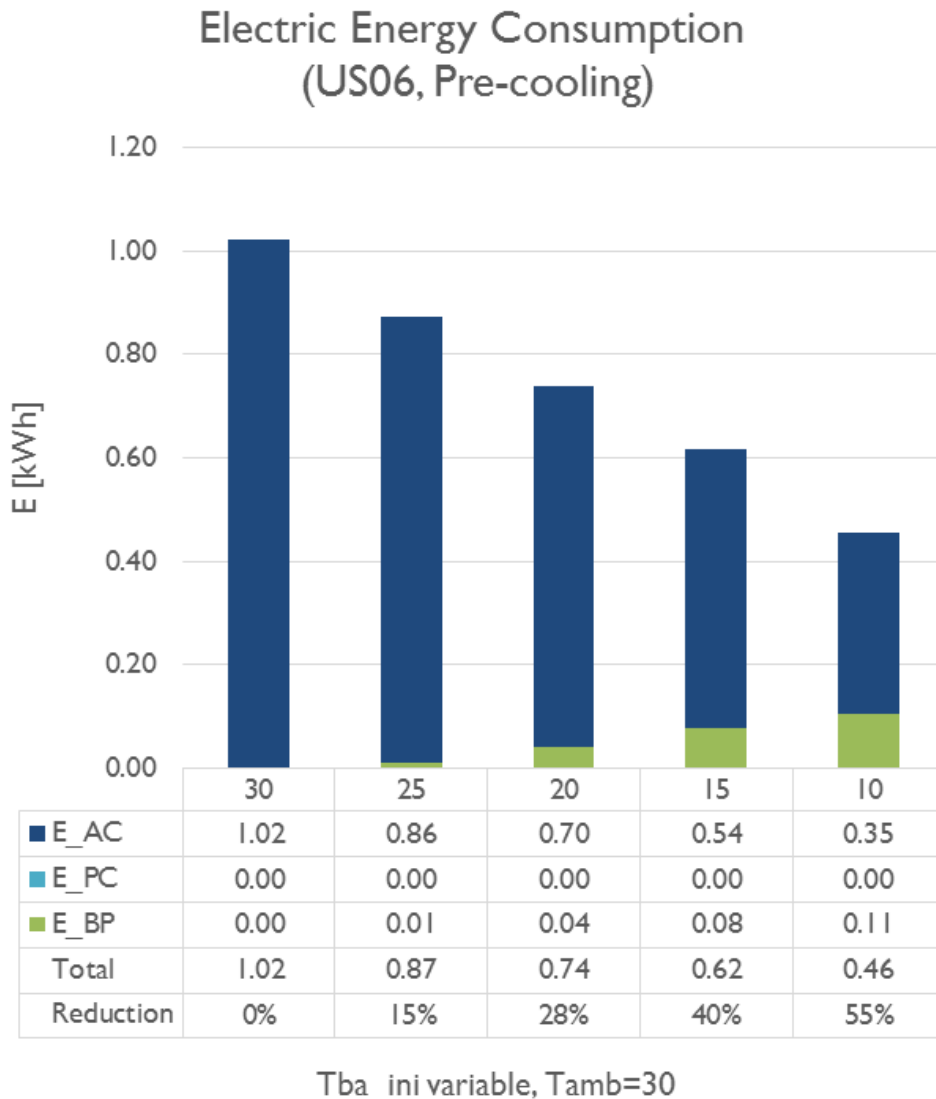


Figure 5.8 Energy saving by the pre-cooling for US06.

Figure 5.9 shows a summary of energy saving by pre-conditioning (pre-heating or pre-cooling). The ambient temperature varied from -20 °C until to 30 °C. The orange columns represent the electricity consumption when there was no pre-conditioning applied. The green columns represent the electricity consumption after mild pre-conditioning was applied. The mild pre-conditioning is defined as the pre-heating to 0 °C when the ambient temperature was lower than 0 °C and the pre-cooling to 20 °C when the ambient temperature was higher than 20 °C. For all cases, the electricity consumption after pre-conditioning applied was below 1 kWh, which was only about 5% of total available battery capacity.

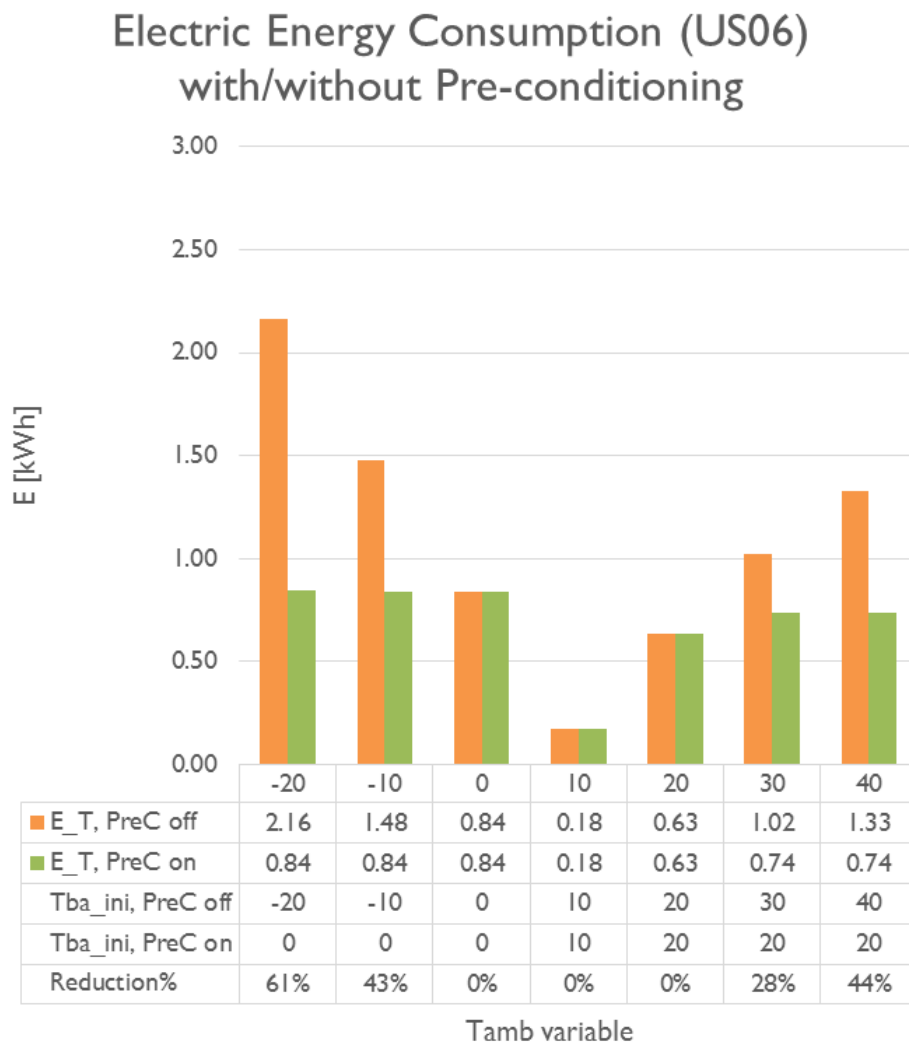


Figure 5.9 Energy saving by the pre-conditioning for US06.

5.1.3 Mild Weather

In mild weather, the total electricity consumption was relatively low compared to that in hot or cold weather. Here the influence of the desired temperature was further investigated. The diagram left in the following figure shows the result at the variable ambient temperature and the fixed desired temperature of 25 °C. When the ambient temperature was at 10 °C or 15 °C, battery temperature was below 25 °C in the whole TDC and thus BTMS stayed in the bypass state. Only when the ambient temperature rose to 20 °C, passive cooling was active and a little more energy was consumed. In comparison to that, the result for the desired temperature of 20 °C were very different. Firstly, the passive cooling was activated in advance even at the ambient temperature of 15 °C. Moreover, at the ambient temperature of 20 °C the passive cooling was invalid and active cooling was required in order to cool down the battery below 20 °C. In conclusion, the desired temperature will obviously affect total electricity consumption. In mild weather, it could be estimated that the higher desired temperature the less total electricity was consumed. However, the desired temperature was set up according the battery feature. Safety, performance and lifespan should also be considered. Further investigation about setting of the desired temperature will reveal more details about its influence.

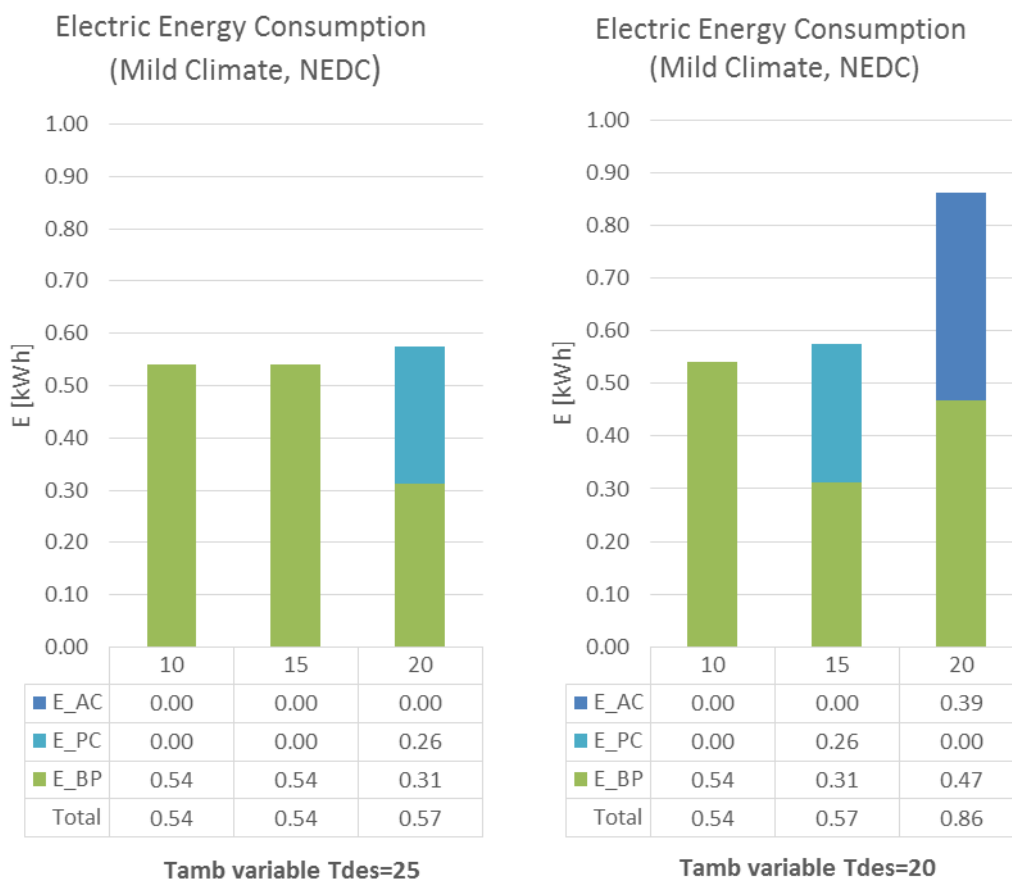


Figure 5.10 Electricity Consumption in mild weather for NEDC, $T_{des}=25/20$ °C.

5.2 PCM Model

PCM uses latent heat to reduce the energy consumption and delay the increase of temperature which was verified through the simulation. Further, the results are compared to those of liquid cooling system in order to find out the advantages and disadvantages of PCM system.

5.2.1 Comparison of Two Systems

Under different conditions the temperature was kept at 23 °C due to phase change with latent heat increasing from 0 to the maximum value, see [Appendix D](#). Furthermore, PCM duration is shown in Table 5.1. The PCM duration accounts for a large proportion of the whole driving time which lasted for around 5000 seconds

Table 5.1 The comparison of energy consumption in liquid cooling system with and without PCM during US06 driving cycle.

T_ _{des}	T_ _{amb}	T_ _{ba_in}	E_ _{total} PCM (kWh)	E_ _{total} Liquid (kWh)	E_ _{saved} (kWh)	E_ _{saved} (%)	PCM Duration (s)
25	0	0	0.8724	0.8408	-0.0316	-3.8%	1693
25	10	10	0.1716	0.1750	0.0034	2.0%	1813.8
25	20	20	0.3733	0.6331	0.2598	41.0%	2365.9
25	30	30	1.0274	1.0230	-0.0044	-0.4%	0
25	30	22.9	0.5235	0.8308	0.3073	37.0%	2474.9
25	40	40	1.3423	1.3258	-0.0165	-1.2%	0
25	40	22.9	0.5235	0.8308	0.3073	37.0%	2474.8

When the initial battery temperature exceeded over 23 °C, the energy consumption of PCM system was higher than liquid cooling system. This was because liquid PCM doesn't use the latent heat and PCM increases the overall heat capacity. Whereas when the initial battery temperature was below the melting point, PCM used the latent heat to absorb the heat from battery which resulted in the reduction of energy consumption, see Table 5.1.

5.2.2 Choose the PCM Mass

The additional mass of the PCM will increase vehicle weight and at the same time decrease the performance of vehicle. However, PCM can use latent heat to decrease energy consumption of BTMS. So the balance point should be found which is related to the PCM mass and its most profitable point.

Table 5.2 Battery capacity loss with the mass addition

Weight (ton)	Range (km)	Battery capacity (kWh)	Battery capacity loss(kWh)
1.7	203.05	29.5	0
1.71	202.43	29.59035	0.090352
1.72	201.81	29.77217	0.272167
1.73	201.18	30.0489	0.548904
1.74	200.56	30.42197	0.921968
1.75	199.95	30.89363	1.393627
1.76	199.34	31.4686	1.968601
1.77	198.74	32.15105	2.651049
1.78	198.14	32.94777	3.447766
1.79	197.55	33.86507	4.365067
1.8	196.95	34.91395	5.413947

The relationship between mass addition and battery capacity loss was estimated according to range loss, see Table 5.2.

PCM of various mass were used to test BTMS energy consumption through model simulation. Further, the energy saving can be calculated by comparing with BTMS energy consumption of liquid cooling system, see Table 5-3, Table 5-4, Table 5-5, Table 5-6.

Table 5.3 Ambient temperature and initial battery temperature of 20 °C during driving cycle US06, the energy benefit and loss.

mass	E_total	E_benefit	E_cost	ΔE	Percentage
0	0.63	0.00	0.00	0.00	0%
10	0.52	0.11	0.09	0.02	3%
20	0.36	0.27	0.27	0.00	0%
30	0.22	0.42	0.55	-0.13	-21%
40	0.17	0.46	0.92	-0.46	-73%
50	0.17	0.46	1.39	-0.93	-147%

Table 5.4 Ambient temperature of 30 °C and initial battery temperature of 22.9 °C during driving cycle US06, the energy benefit and loss.

mass	E_total	E_benefit	E_cost	ΔE	Percentage
0	0.83	0.00	0.00	0.00	0%
10	0.65	0.18	0.09	0.09	10%
20	0.49	0.34	0.27	0.07	8%
30	0.33	0.50	0.55	-0.05	-6%
40	0.22	0.62	0.92	-0.31	-37%
50	0.17	0.66	1.39	-0.73	-88%

Table 5.5 Ambient temperature and initial battery temperature of 20 °C during driving cycle NEDC, the energy benefit and loss.

mass	E_total	E_benefit	E_cost	ΔE	Percentage
0	0.57	0.00	0.00	0.00	0
5	0.55	0.03	0.05	-0.02	-3%
10	0.54	0.03	0.09	-0.06	-10%
20	0.54	0.03	0.27	-0.24	-42%
30	0.54	0.03	0.55	-0.52	-90%

Table 5.6 Ambient temperature of 30 °C and initial battery temperature of 22.9 °C during driving cycle US06, the energy benefit and loss.

mass	E_total	E_benefit	E_cost	ΔE	Percentage
0	0.80	0.00	0.00	0.00	0
5	0.73	0.07	0.05	0.03	3%
10	0.61	0.19	0.09	0.10	12%
15	0.54	0.26	0.18	0.08	10%
20	0.54	0.26	0.27	-0.01	-1%
25	0.54	0.26	0.41	-0.15	-18%

From the tables above, it can be seen that when PCM mass was 10kg, the difference between benefited energy and energy loss was the biggest. So 10kg was chosen as optimal PCM mass.

6 Conclusion

Generally, the two models for the two proposed systems have been built up fulfilling almost all the requirements asked for in the beginning. Numerical results with figures have been generated under different weather, control and driving conditions. The electric energy consumption predicted makes sense and had the correct tendency. Moreover, the modelling showed also its flexibility to fit new systems with a few modification.

CLS model results have indicated how the driving behaviour, battery initial temperature and ambient temperature influenced the BTMS and the corresponding electricity consumption. From the results it was seen that different driving cycles would change the BTMS feature significant in hot weather but less significantly in cold weather. The ambient temperature was the most important variable for the BTMS. The battery initial temperature representing pre-conditioning treatment changed the energy consumption significantly, especially in extreme hot and cold weather.

The PCM model showed that the electric range of EV was sensitive to the vehicle mass. PCM could bring significant improvement of BTMS, but the mass of PCM was difficult to choose. For this specific case, 10 kg of PCM was an optimal point. However, further investigation is still required to figure out the influence in detail.

7 Future Prospects

Though a Simulink model has been built up, a lot more work could be done in the topic of battery thermal management system. Firstly, this investigation as the first study focused more on the essential issues, such as system requirements and modelling functions. Thus, only a simplified model has been completed. This model has low accuracy and lacks validation with laboratory data. Another limitation of this thesis is the connection and coupling with other models. Currently this model can only process static data from file. The interface of the model should be therefore further developed to interact with other models of battery pack or vehicle components. Last but not least, optimisation of the thermal management system can also be achieved by pre- and post-conditions, different control strategies, customer behaviour and other factors.

Accuracy improvement

In the Simulink model only main heat sources and heat sinks are included for calculation. The following factor may also have an effect:

- Heat transfer through the insulation material of battery pack case
- Heat dissipation from electric inverter, electric control unit and water pump

Also, many components could be improved to achieve a better prediction of energy balancing and energy consumption:

- Use CFD Simulation tools to predict the heat transfer condition of radiator, chiller and battery pack. The heat transfer between thermal fluid and battery cells should be thoroughly investigated.
- The pressure drop of each component and pipe should be added together and then the calculations of water pump power will be more accurate.
- Dynamic performance of heater, chiller and radiator could be introduced instead of the current static performance in order to improve the prediction, especially during start-up period and sudden power changes.
- Laboratory tests of the same BTMS system could be carried out. A comparison between modelling result and experimental data could further correct the error of the modelling.

Functionality Development

There are several points which could be extended in the future development:

- One of the high-priorities is to connect this Simulink model with available thermodynamic simulation tools such as GT-SUITE or StateFlow in order to achieve more accurate heat-transfer calculation.
- Also, a direct connection with the battery electro-thermal model is also needed to output the power of BTMS and to obtain the dynamic data of battery heat generation rate instead of static data.
- Another important part of BTMS is to monitor the battery thermal health in order to prevent battery from thermal issues and damage. It is important to send a warning in risk situations and to send an emergency stop signal when the system is in danger.

Alternative work

Beside the two topics above, the following points are also very interesting:

- **Pre- and post-conditioning**
The most interesting potential energy-saving that should be further investigated is the battery behaviour before and after driving and the corresponding thermal treatment i.e. pre- and post-condition, which should be implemented by BTMS. The different control strategy can be developed according to different conditions. Both heating and cooling energy consumption will change and could be saved.
- **Control strategy of BTMS for charging cycle**
During charging, the battery pack will also generate a large amount of heat requiring even more strict thermal demands. To develop a proper control strategy of BTMS for charging is highly recommended to ensure both safety and high charging rate.
- **Control strategy optimization**
This thesis has generally analysed the increasing energy consumption with decreasing the desired temperature of the battery, which is charged by control unit. But there are some other factors affecting on the energy consumption of BTMS, such as the switching differential of control relays for radiator and air conditioner.
- **Measurement, analysis and improvement of battery temperature unevenness**
In this thesis the battery was treated as a homogenous body. Each point on battery simultaneously had the same temperature, but in reality battery cells have a different temperature distribution. To measure this is interesting. It is also interesting to reduce the unevenness by re-design of the BTMS.
- **BTMS simulation with customised conditions**
Evaluation of BTMS energy consumption is related not only to one given condition but on a combination of different situations. For example, both cold winter and hot summer conditions should be included for a comprehensive evaluation. It is reasonable to develop such simulation conditions with varying parameters, such as the whole year ambient temperatures in a city, charging behaviour, and BTMS ageing. This overall evaluation would present a more practical performance of BTMS

References

- Battery University, 2014. *Battery University*. [Online]
Available at: http://batteryuniversity.com/learn/article/types_of_lithium_ion
[Accessed 08 04 2014].
- Binder, 2014. *Thermoelectric cooling technology*. [Online]
Available at: <http://www.binder-world.com/ext/getdownload.cfm?pub=74&lang=2>
[Accessed 06 03 2014].
- Charged, 2014. *Charged electric vehicles magazine*. [Online]
Available at: <http://chargedevs.com/features/allcell-technologies%E2%80%99-new-phase-change-thermal-management-material/>
[Accessed 20 04 2014].
- CW, 2013. *Chevy Volt battery pack: Rugged but precise*. [Online]
Available at: <http://www.compositesworld.com/articles/chevy-volt-battery-pack-rugged-but-precise>
[Accessed 25 03 2014].
- Digikey, 2014. *Digikey*. [Online]
Available at: <http://www.digikey.com/Web%20Export/Supplier%20Content/api-technologies-1171/pdf/api-ptc-applications.pdf?redirected=1>
[Accessed 23 05].
- Eberspracher, 2014. *Eberspracher*. [Online]
Available at: <http://www.eberspracher.com/products/electrical-heaters.html>
[Accessed 02 03 2014].
- electropaedia, 2014. *electropaedia*. [Online]
Available at: <http://www.mpoweruk.com/chemistries.htm>
[Accessed 19 05 2014].
- Electropaedia, 2014. *Lithium Battery Failures*. [Online]
Available at: http://www.mpoweruk.com/lithium_failures.htm
[Accessed 06 03 2014].
- GM-Volt, 2010. *The chevrolet volt cooling/heating system explained*. [Online]
Available at: <http://gm-volt.com/2010/12/09/the-chevrolet-volt-coolingheating-systems-explained/>
[Accessed 24 03 2014].
- Gripumps, 2014. *Gripumps*. [Online]
Available at: <http://www.gripumps.com/series.asp?action=display&id=172>
[Accessed 03 04 2014].
- Huairui, 2014. *200W Communication Battery Industry Cabinet Thermoelectric Cooler (TEC)*. [Online]
Available at: http://huaruicooling.en.alibaba.com/product/683329653-215080785/200W_Communication_Battery_Industry_Cabinet_Thermoelectric_Cooler_TEC_.html
[Accessed 06 03 2014].
- Incropera, F. P., 2007. *Fundamentals of Heat and Mass Transfer*. 6th edition ed. s.l.:John Wiley & Sons.

- Kizilel, R., Sabbah, R., Selman, J. Robert & Al-hallaj, S., 2009. An alternative cooling system to enhance the safety of Li-ion battery packs. *Journal of Power Sources*, 194(2), pp. 1105-1112.
- Lauda, 2014. *Lauda*. [Online]
Available at:
http://www.lauda.de/hosting/lauda/website_en.nsf/urlnames/prospektdownload
[Accessed 08 04 2014].
- Matthe, R., Turner, L. & Mettlach, H., 2011. VOLTEC Battery System for Electric Vehicle with Extended Range. *SAE International Journal of Engines*, 4(1), pp. 1944-1962.
- Mc Nally Institute, 2014. *Mc Nally Institute*. [Online]
Available at: <http://www.mcnallyinstitute.com/14-html/14-04.htm>
[Accessed 07 04 2014].
- Peng Zhou, E. C. C., 2010. *Electric vehicle thermal management system*. US, Patent No. US 2010/0025006 A1.
- Pesaran, A. A., 2001. Battery Thermal Management in EVs and HEVs : Issues and Solutions. *Advanced Automotive Battery Conference*, p. 10.
- Pesaran, A. A., 2002. Battery thermal models for hybrid vehicle simulations. *Journal of power sources*, Volume 110(2), p. 377–82.
- Ricker, N. L., 2014. *A Simulink Tutorial*. [Online]
Available at: tang.eece.wustl.edu/SimulinkTutorial.pdf
[Accessed 16 05 2014].
- Sabbah, R., Kizilel, R., Selman, J. R. & Al-Hallaj, S., 2008. Active (air-cooled) vs. passive (phase change material) thermal management of high power lithium-ion packs: Limitation of temperature rise and uniformity of temperature distribution. *Journal of Power Sources*, 182(2), pp. 630-638.
- Spirax Sarco, 2011. *The Steam and Condensate Loop*. s.l.:s.n.
- Tran, T.-H. e. a., 2014. Experimental investigation on the feasibility of heat pipe cooling for HEV/EV lithium-ion battery. *Applied Thermal Engineering*, 2(63), p. 551–558.
- Valeo, 2010. *Battery Thermal Management for HEV & EV – Technology overview*. s.l., s.n.

Appendix A: System Evaluation

Appendix A1: Concept Selection Matrix

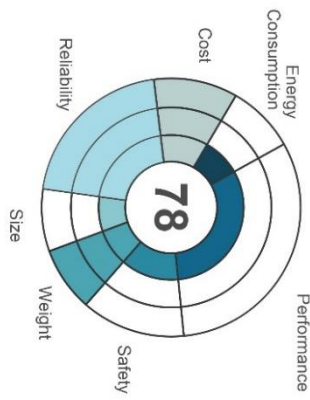
System Characteristic	Air		Coolant			Refrigerant cooling system	PCM-graphite	Heat pipe	Thermoelectrics
	active cooling	passive cooling	active cooling	combination	cooling system				
Cooling power	small	medium	large	large	large	large	large	medium	medium
Temperature distr.	uneven	uneven	even	even	even	even	even	moderate	moderate
Propagation of thermal runaway	big	big	small	small	small	small	small	big	big
Heat transfer Efficiency	low	high	high	high	high	medium	high	medium	low
Heating (available)	yes	no	yes	yes	yes	yes	yes	no	yes
Cooling (available)	yes	yes	yes	yes	yes	yes	yes	yes	yes
Weight	light	medium	heavy	heavy	heavy	medium	medium	medium	light
Size	large	small	small	small	small	small	small	large	small
Complexity	simple	complex	complex	complex	complex	complex	medium	moderate	simple
Ease of Maintenance	easy	difficult	difficult	difficult	difficult	difficult	easy	moderate	easy
Reliability	high	medium	low	low	low	low	low	high	easy
BTMS Lifetime	long	moderate	moderate	moderate	moderate	moderate	long	long	short
First cost	low	medium	high	high	high	high	moderate	high	high
Annual cost	low	medium	high	high	high	high	low	moderate	high
Energy consumption	high	low	low	low	moderate	low	even low	high	high
Ventilation	good	medium	medium	medium	medium	medium	bad	good	bad

Appendix A2: Evaluation Score Table of different BTMS

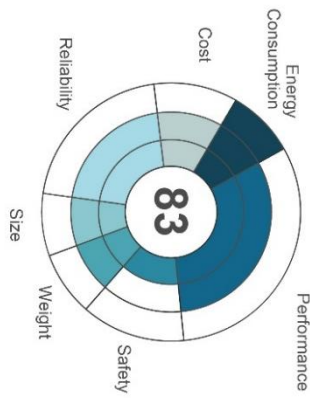
Items	Performance	Safety	Weight	Size	Reliability	Cost	Energy Consumption	Sum
Weighting factor	x12	x5	x3	x3	x11	x4	x4	
Active Air system	1	1	3	1	3	3	1	78
Passive Liquid System	2	1	2	2	2	2	3	83
Active Liquid System	3	3	1	3	1	1	2	86
Combined Liquid System	3	3	1	3	1	1	3	90
Direct Refrigerant System	3	2	2	3	1	1	3	88
PCM	3	3	2	3	1	1	3	93
Heat pipe	2	2	2	1	2	2	1	77
Thermoelectrics	2	1	3	3	2	1	1	77

Appendix A3: Evaluation Diagrams of different BTMS

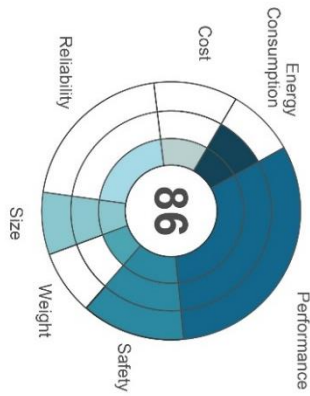
Active Air System



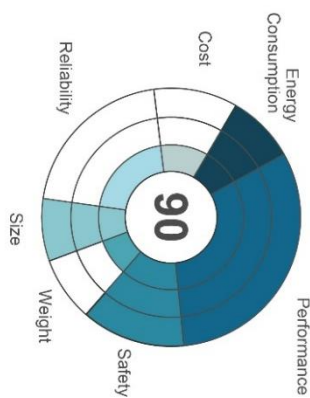
Passive Liquid System



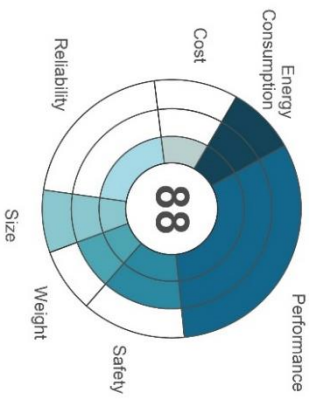
Active Liquid System



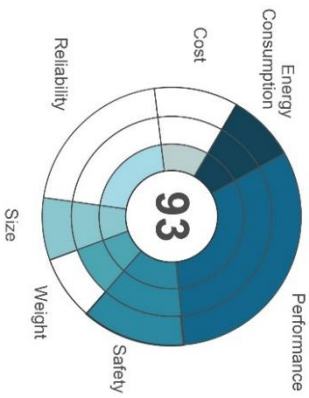
Combined Liquid System



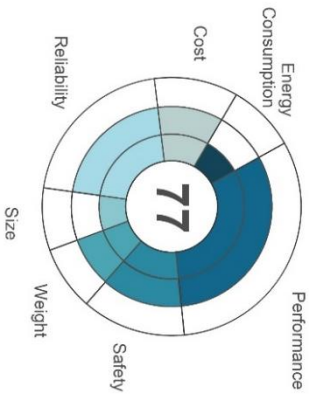
Direct Refrigerant System



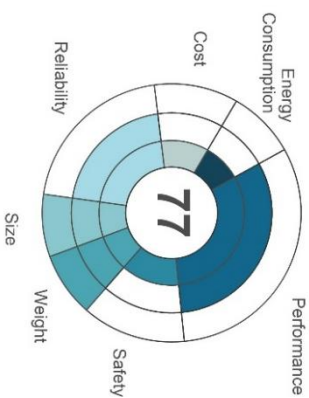
PCM

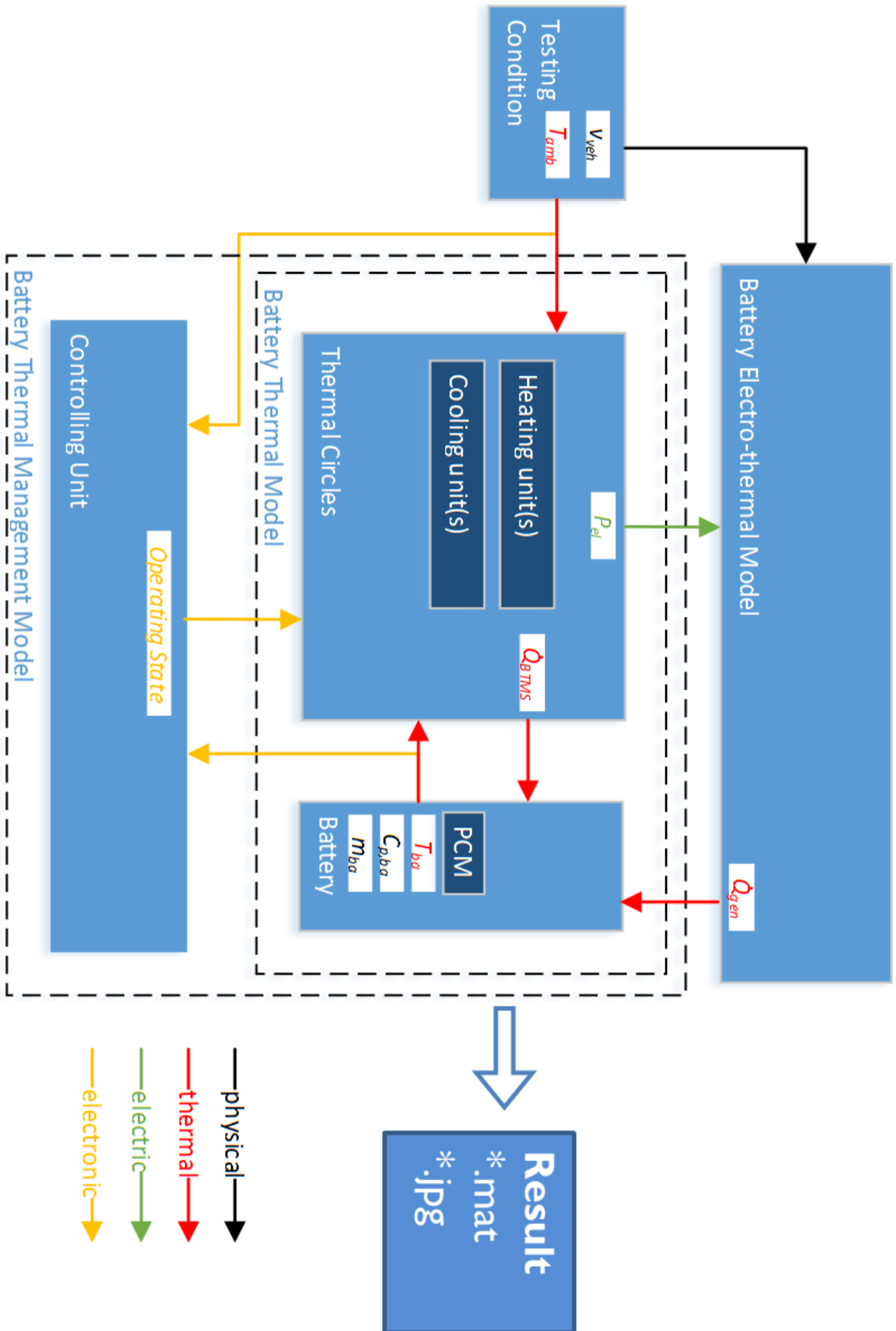


Heat Pipe

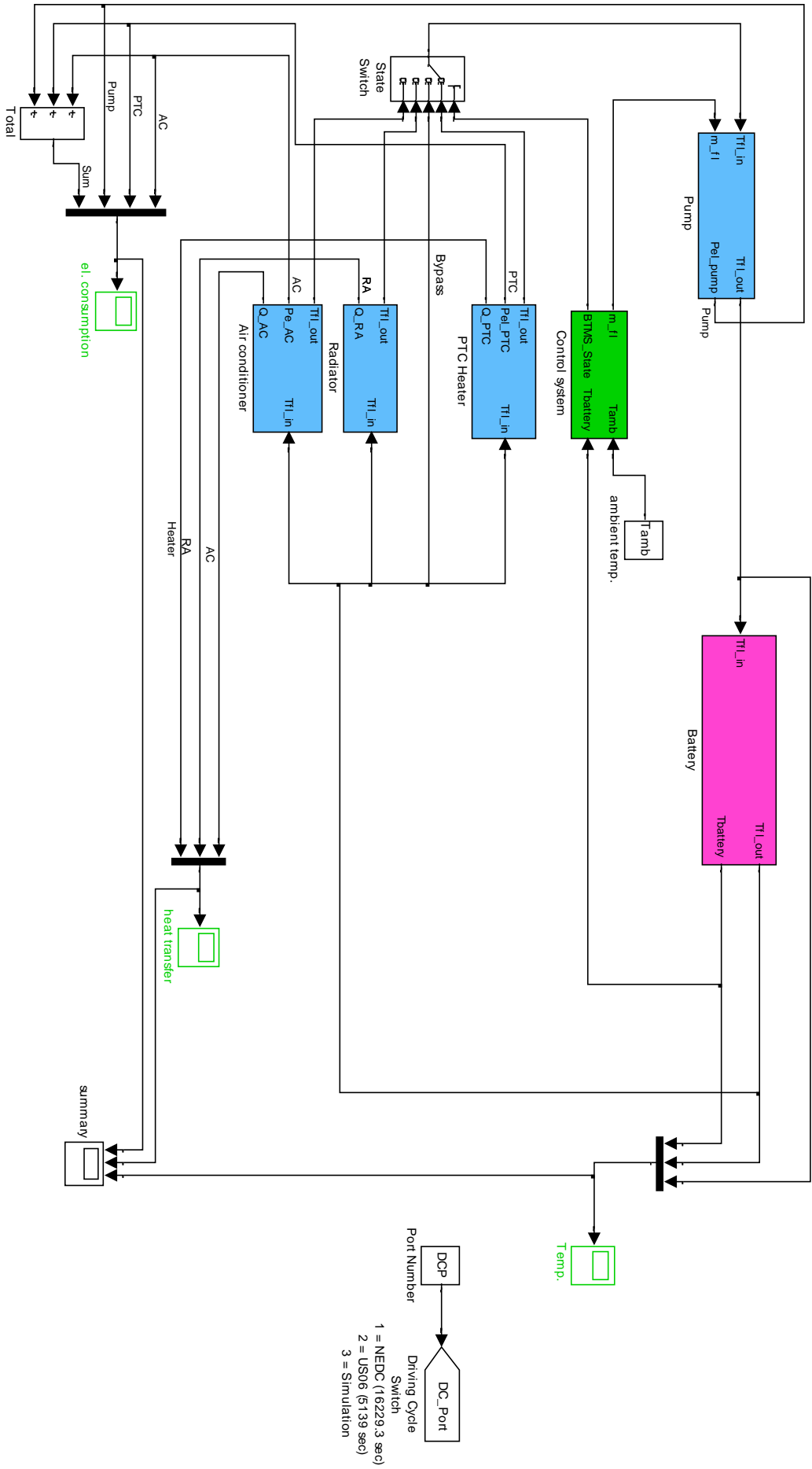


Thermoelectrics

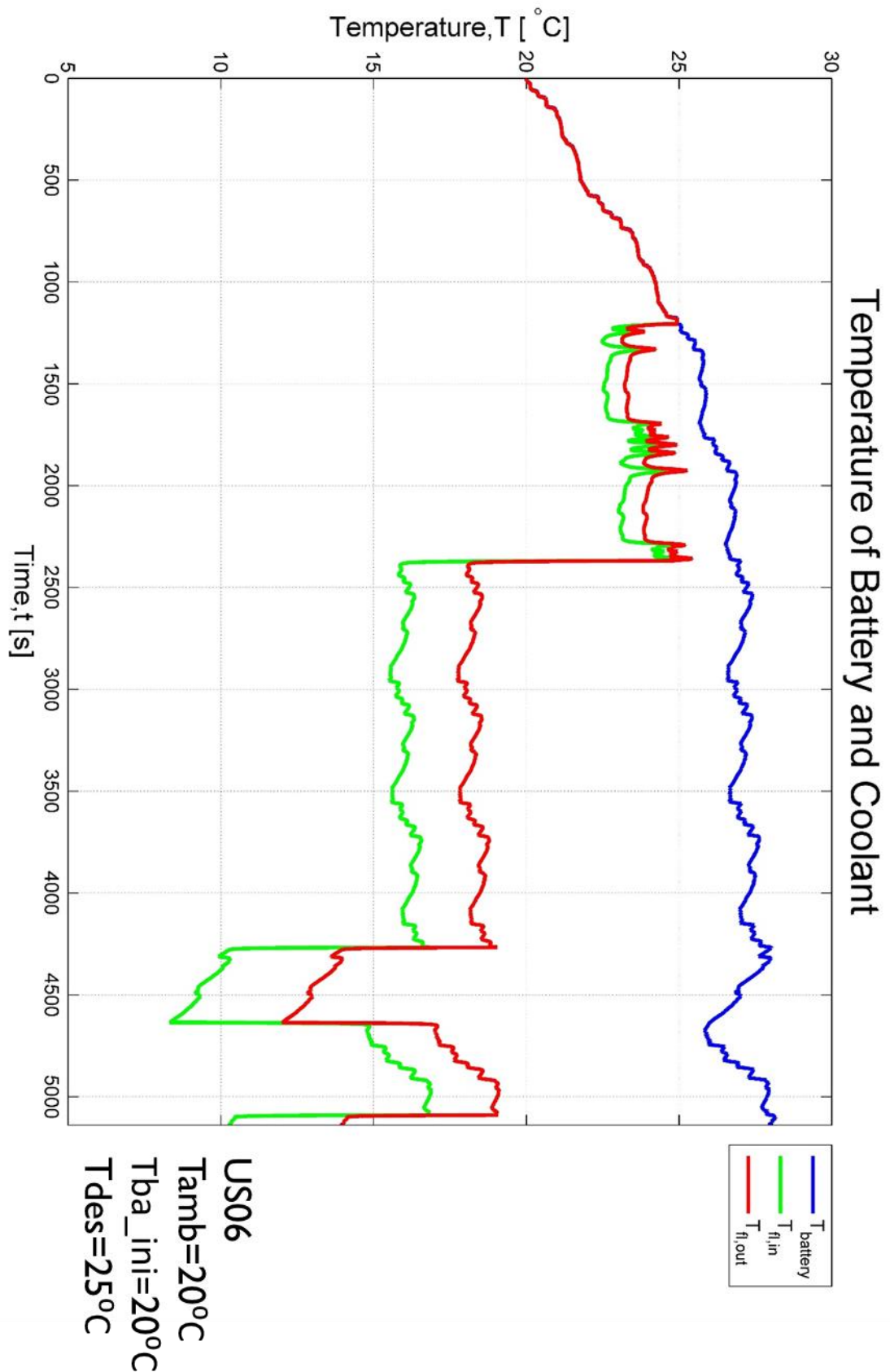




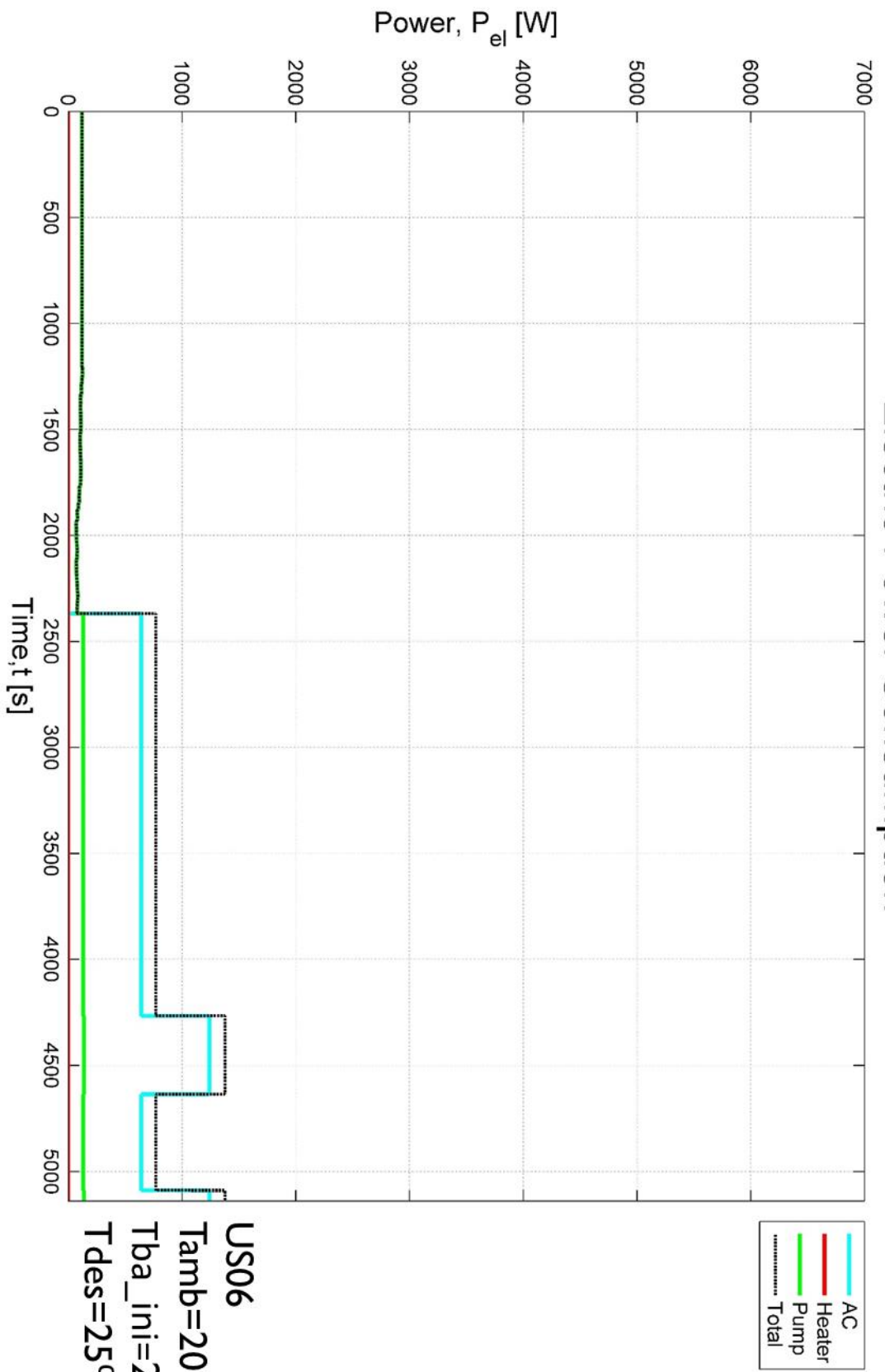
Appendix B2: MATLAB/Simulink Modelling Process



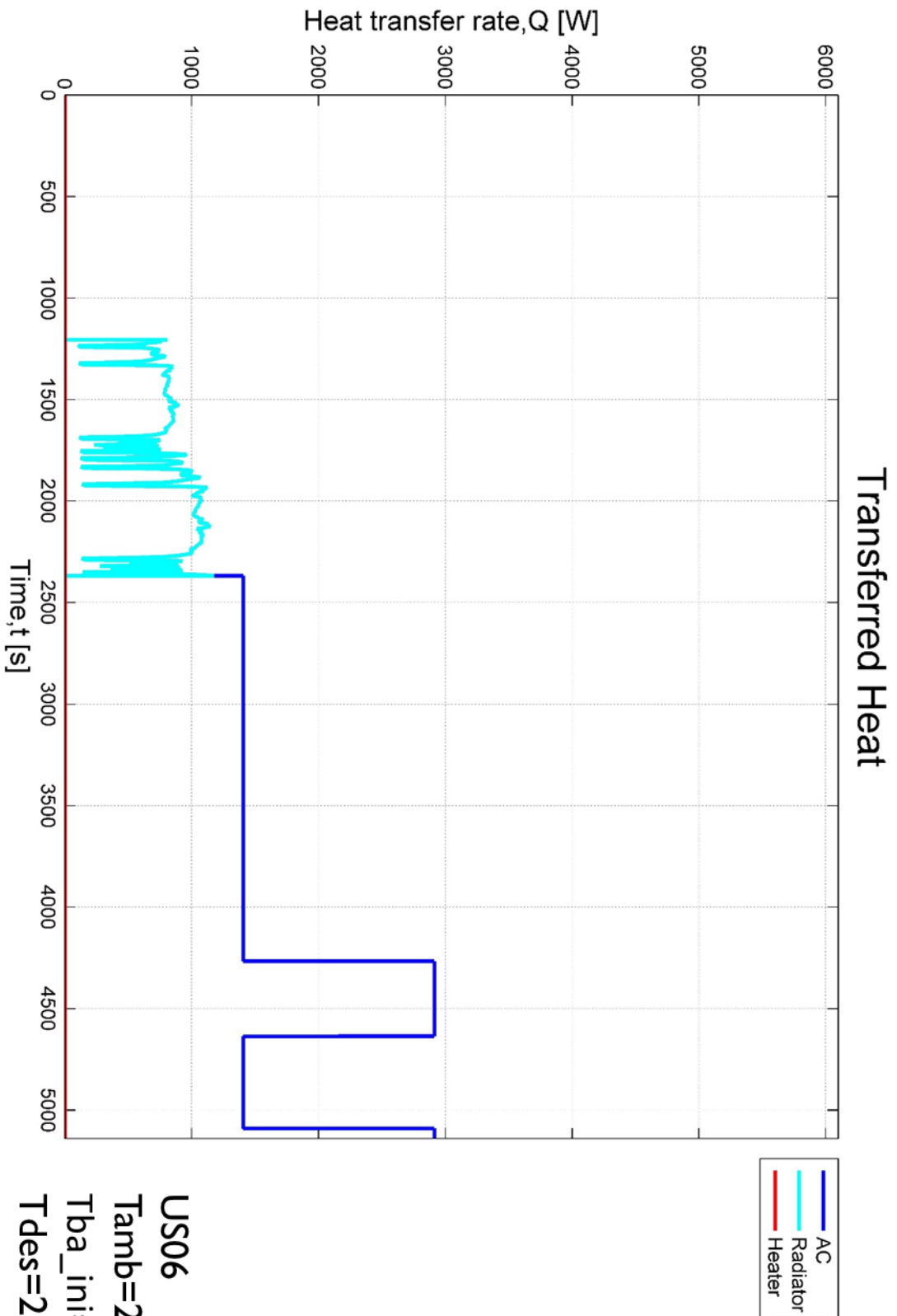
Appendix C: CLS Results

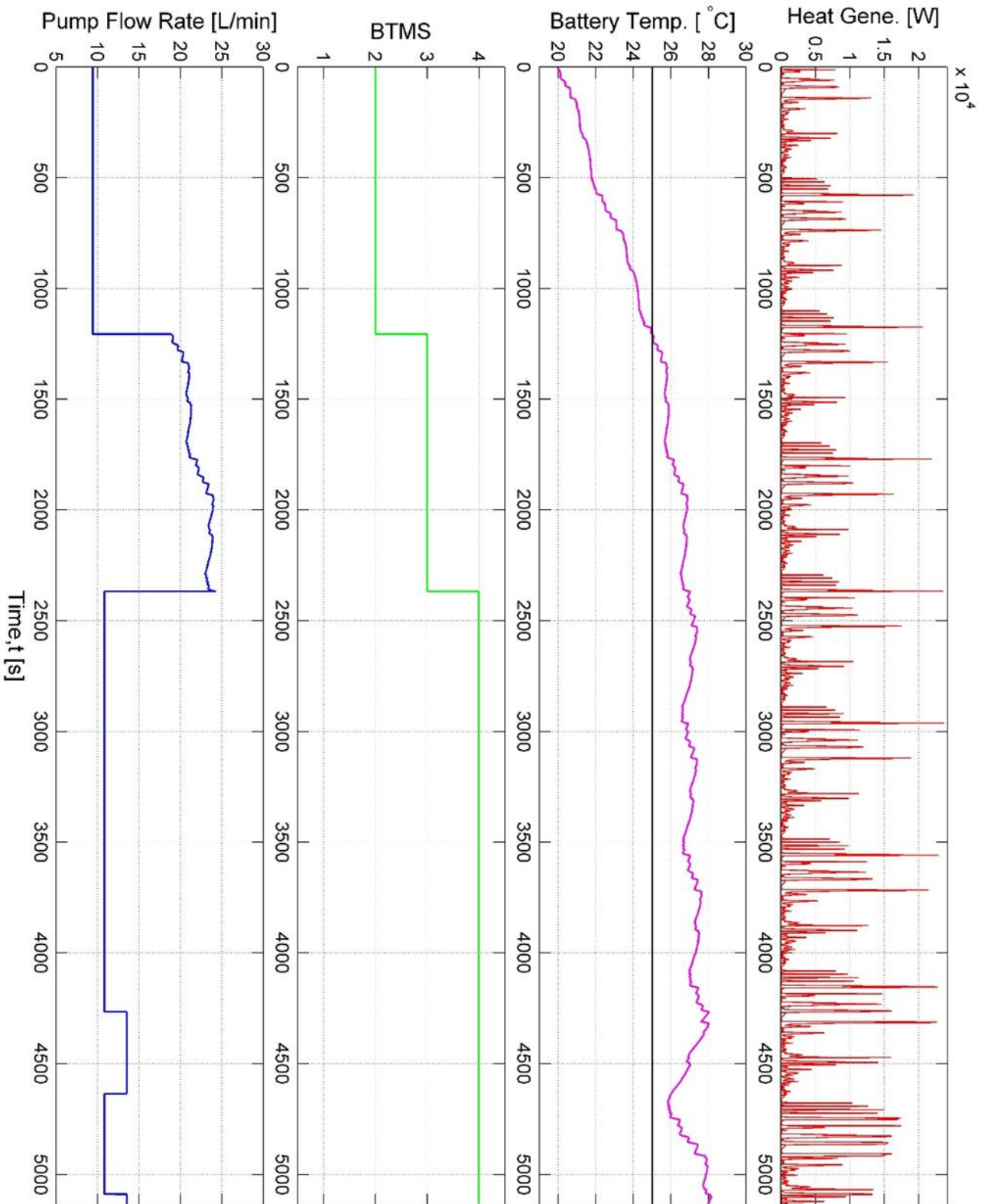


Electric Power Consumption



US06
 $T_{amb}=20^{\circ}\text{C}$
 $T_{ba_ini}=20^{\circ}\text{C}$
 $T_{des}=25^{\circ}\text{C}$



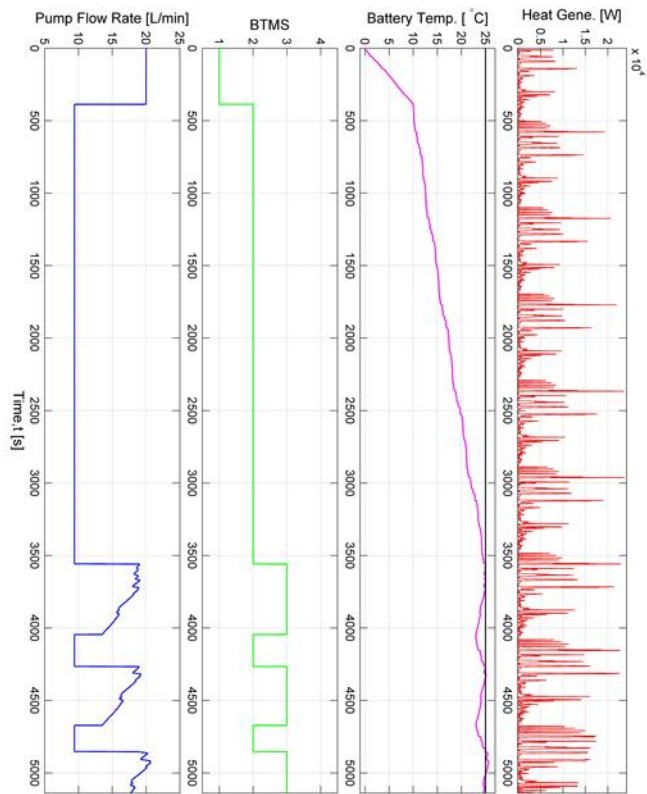


US06
Tamb=20°C
Tba_ini=20°C
Tdes=25°C

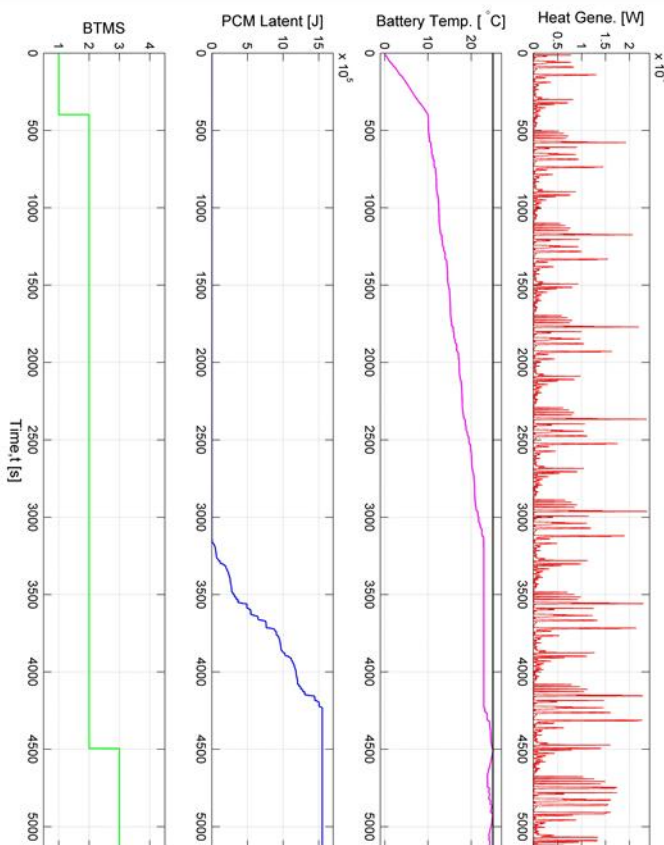
Appendix D: CLS+PCM Results

Appendix D1: Comparison of results between two systems when $T_{amb}=T_{ba_in}=0^{\circ}\text{C}$

CLS

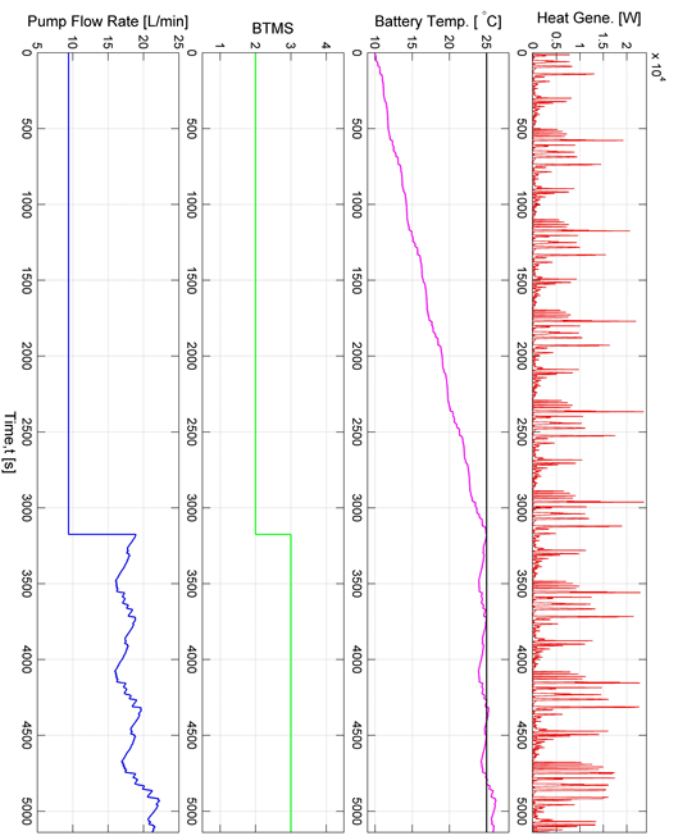


CLS+PCM

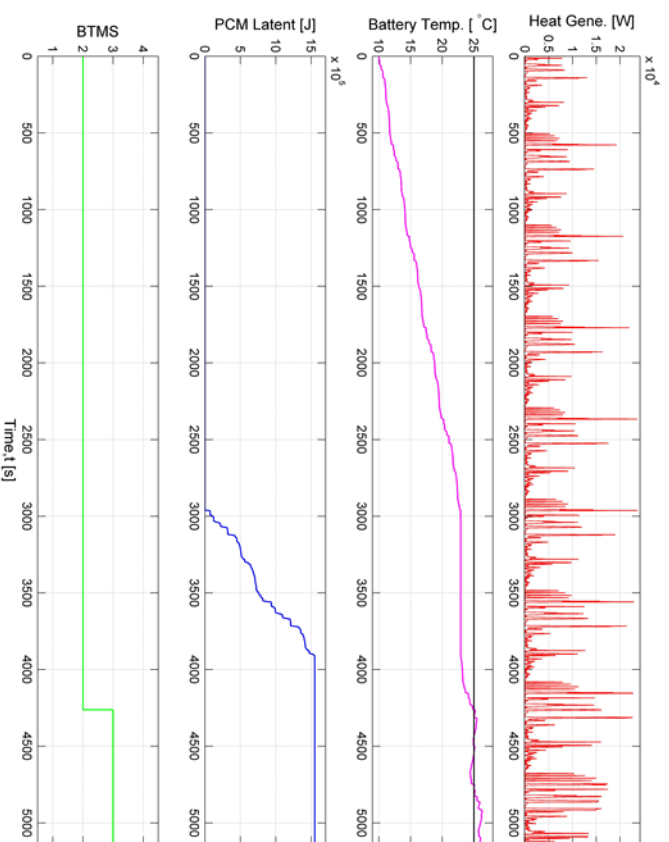


Appendix D2: Comparison of results between two systems when $T_{amb}=T_{ba_in}=10^{\circ}C$

CLS

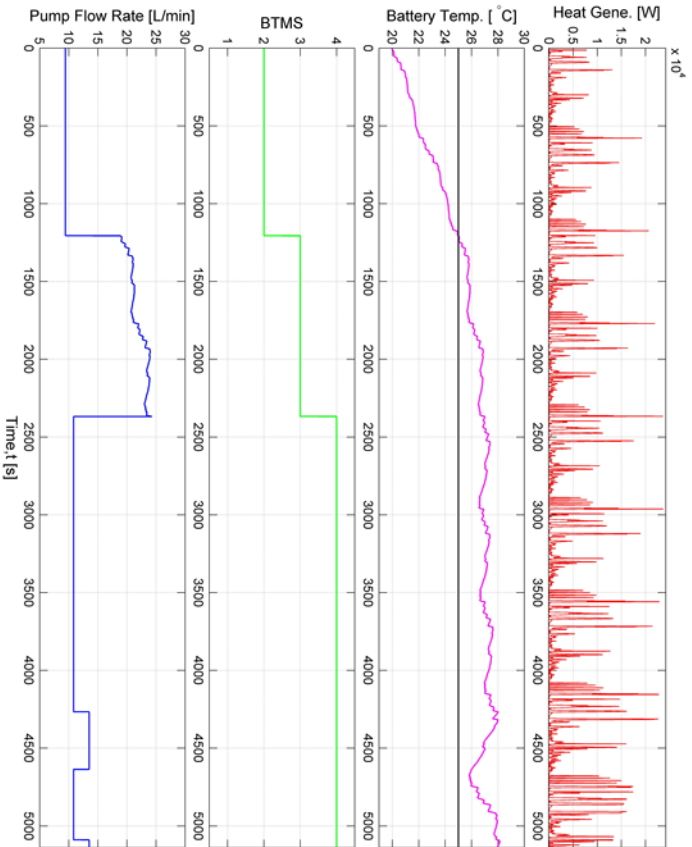


CLS+PCM

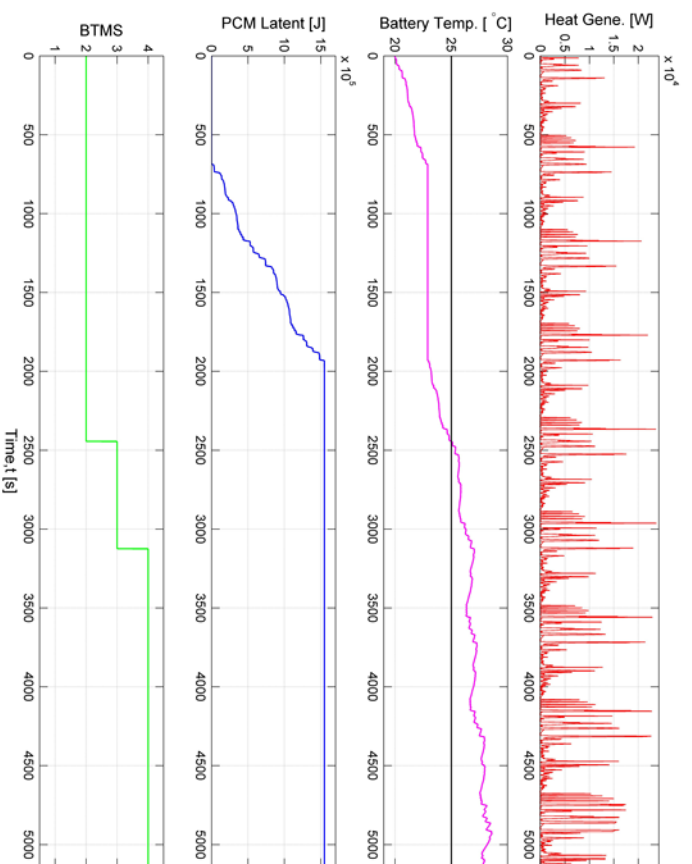


Appendix D3: Comparison of results between two systems when $T_{amb}=T_{ba_in}=20^{\circ}\text{C}$

CLS

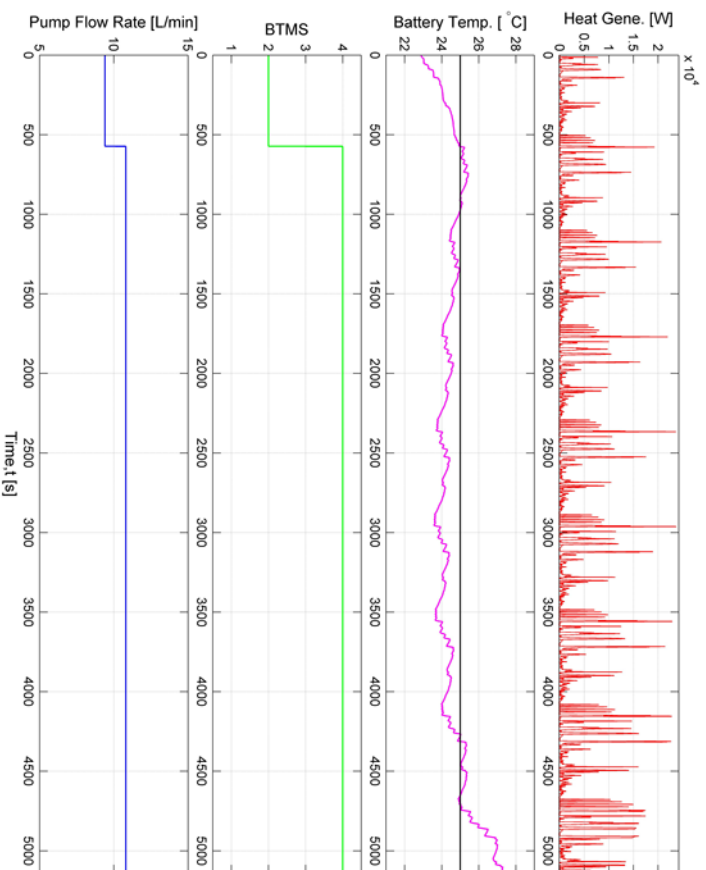


CLS+PCM

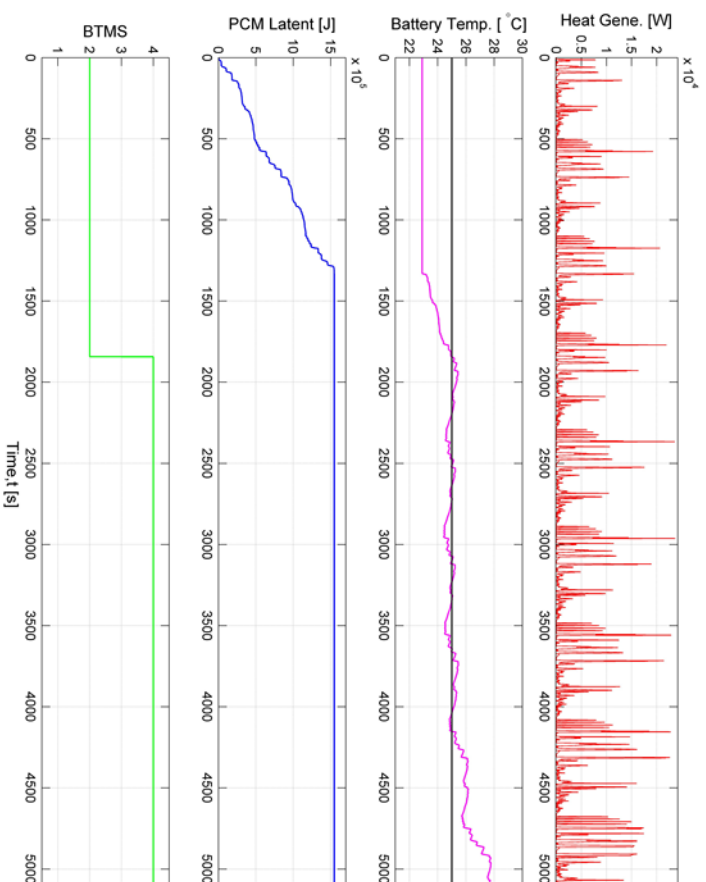


Appendix D4: Comparison of results between two systems when $T_{amb}=30^{\circ}\text{C}$ $T_{ba_in}=22.9^{\circ}\text{C}$

CLS

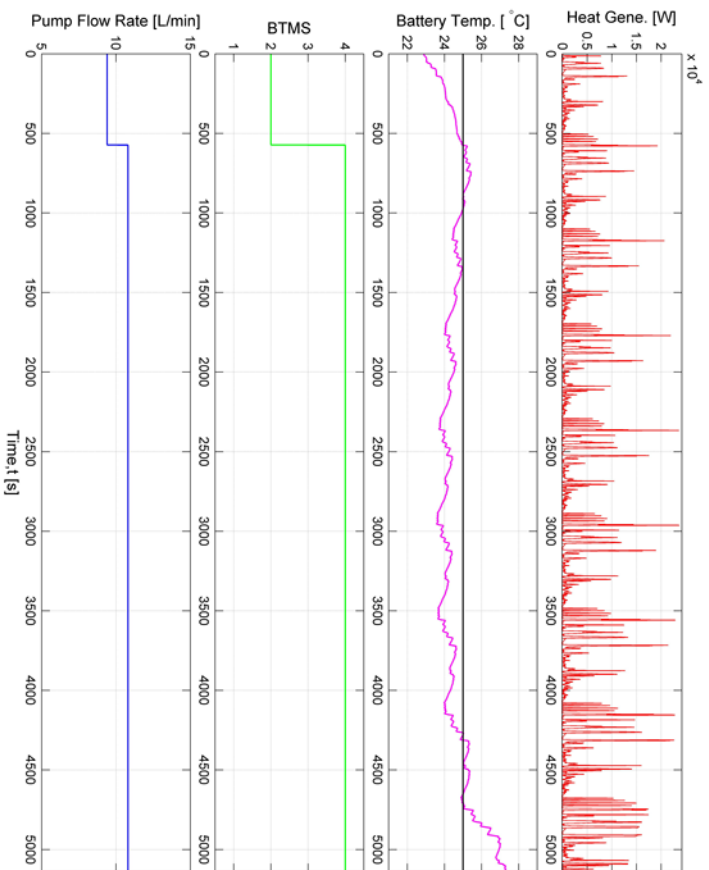


CLS+PCM



Appendix D5: Comparison of results between two systems when $T_{amb}=40^{\circ}\text{C}$ $T_{ba_in}=22.9^{\circ}\text{C}$

CLS



CLS+PCM

